Histone binding of ASF1 is required for fruiting body development, but not for genome stability in the filamentous fungus *Sordaria macrospora*

Jan Breuer[1], Tobias Busche[2,3], Jörn Kalinowski[2], Minou Nowrousian[1]

[1]Department of Molecular and Cellular Botany, Ruhr University Bochum, 44801 Bochum, Germany
[2]Center for Biotechnology, Bielefeld University, 33594 Bielefeld, Germany
[3]Medical School OWL, Bielefeld University, 33615 Bielefeld, Germany

running title:
ASF1 in fungal development

author for correspondence:
Minou Nowrousian
Department of Molecular and Cellular Botany
Ruhr University Bochum
Universitaetsstr. 150
44801 Bochum
minou.nowrousian@rub.de

Abstract

The highly conserved eukaryotic histone chaperone ASF1 is involved in the assembly and disassembly of nucleosomes during transcription, DNA replication and repair. It was the first chaperone discovered to be involved in all three of these processes. The filamentous fungus *Sordaria macrospora* is one of only two multicellular organisms where *asf1* deletions are viable, which makes it useful for *in vivo* analysis of this central regulator of eukaryotic chromatin structure. Deletion of *asf1* in *S. macrospora* leads to sterility, a reduction of DNA methylation, and upregulation of genes that are usually weakly expressed in the wild type. Here, we focused on the functions of the highly conserved core and the divergent C-terminal tail of ASF1, studied the effects of ASF1 on histone modifications and tested its relevance for genomic stability. By Co-IP and complementation analysis we showed that substitutions of amino acid V94 or truncations of the C-terminal tail abolish histone binding and do not complement the sterile mutant phenotype. Δasf1 is sensitive to the DNA damaging agent MMS, while complementation strains, even those with non-histone-binding variants, regain wild type-like resistance. To aid in subsequent ChIP-seq and Hi-C analyses, we generated a chromosome-resolved genome assembly of *S. macrospora*. ChIP-Seq analysis revealed a global increase of H3K27me3 in Δasf1, accompanied by a global decrease of H3K56ac. By using Hi-C we detected a tandem duplication of around 600 kb on chromosome 2 in the mutant. Crossing experiments indicated linkage between the viability of Δasf1 strains and the presence of the duplication.

Importance

Histone chaperones are proteins that are involved in nucleosome assembly and disassembly and can therefore influence all DNA-dependent processes including transcription, DNA replication and repair. ASF1 is a histone chaperone that is conserved throughout eukaryotes. In contrast to most other multicellular organisms, a deletion mutant of *asf1* in the fungus *Sordaria macrospora* is viable; however, the mutant is sterile. In this study, we could show that the histone binding ability of ASF1 is required for fertility in *S. macrospora*, whereas the function of ASF1 in maintenance of genome stability does not require histone binding. We also showed that the histone modifications H3K27me3 and H3K56ac are misregulated in the Δasf1 mutant. Furthermore, we identified a large duplication on chromosome 2 of the mutant strain that is genetically linked to the Δasf1 allele present on chromosome 6, suggesting that viability of the mutant might depend on the presence of the duplicated region.

Introduction

Multicellular development is a complex process that evolved independently in multiple branches of eukaryotes (1). In fungi, multicellular development evolved at least twice and possibly more times, the most prominent examples being the fruiting bodies of filamentous ascomycetes and basidiomycetes (2). To study the genetic background of multicellular development, simple, easy to handle model organisms are of particular interest. Several species of fungi have proven to be usable models for the analysis of developmental processes, and the generation of complex, multicellular fruiting bodies of filamentous ascomycetes is an excellent example (3). *Sordaria macrospora*, a homothallic ascomycete that can form its perithecia in 7 days under laboratory conditions, has been used as a model to study fungal sexual development and multicellular development in general. During the formation of fruiting bodies in *S. macrospora*, at least 13 different cell types are generated, many of which cannot be found in vegetative mycelium (4). Sexual development and perithecia formation are accompanied by transcriptional changes, and transcriptomics can be a helpful tool to identify important developmental genes by reverse genetic approaches. A number of transcription factors and chromatin modifiers have been identified this way and were proven to be fundamental for multicellular development (5). Among them is the conserved histone chaperone ASF1 that was shown to be upregulated during sexual development and is essential for this process in *S. macrospora* (6). ASF1 is involved in the assembly and disassembly of nucleosomes during transcription, replication and DNA-repair and was the first chaperone found to be involved in all three of these processes. It mediates nucleosome assembly and disassembly in promoter regions during transcriptional activation and elongation in *Saccharomyces cerevisiae* (7). ASF1 is also important for histone modification by interacting with enzymes that mediate the corresponding modifications. For example, it has been shown to be involved in the acetylation of histone H3 at lysines 9 and 56 and also to play a role in the genome-wide deacetylation of histones (8, 9). The methylation of histones also appears to proceed in conjunction with ASF1. In *Mus musculus*, an altered distribution of H3K9me3 and H3K27me3 was shown under ASF1 deficiency. ASF1 was also proven to be important for histone recycling (10). Additionally, ASF1-depleted cells were shown to exhibit higher tendencies for double strand breaks, showcasing a role of ASF1 during the maintenance of genomic stability (11). The function and structure of ASF1 is highly conserved in all eukaryotes. The 155 amino acids of the N-terminus of ASF1 form a globular core with conserved acidic patches that mediate interaction with the C-terminus of histone H3. ASF1 has been shown to interact with the histone H3-H4 heterodimer *in vitro* and *in vivo*. In addition to binding of H3, binding of the H4 C-terminus to ASF1 also occurs. ASF1 and the H3-H4 dimer can form a heterotrimeric complex, although both histones can be bound individually by ASF1 (7). The central role of ASF1 for eukaryotic chromatin structure is underscored by findings in human cell lines that showed all non-DNA bound histones H3 and H4 are bound to ASF1 (12, 13). Therefore, researching ASF1 functions during multicellular

93 development might be fundamental for understanding the contribution of the chromatin landscape to
94 development in fungi and multicellular eukaryotes in general. Gaining insight into the functions of ASF1
95 is hindered by the fact that deletions of the respective gene are lethal in almost all higher eukaryotes.
96 Thus, research on ASF1 was mostly conducted with ASF1-depleted cell lines, *in vitro* experiments and
97 studies of the unicellular *S. cerevisiae* where an *asf1* deletion is viable (14-16). *S. macrospora* and
98 *Arabidopsis thaliana* were shown to be exceptions in this regard and deletions are viable in these
99 organisms (6, 17) (for *S. macrospora*, this might depend on the presence of a secondary mutation as
100 described in the results). Therefore, the analysis of *S. macrospora* Δasf1 strains offers the unique
101 opportunity to perform ASF1 research *in vivo* in a multicellular fungus. These strains were shown to be
102 sterile, highlighting a central role of ASF1 during sexual development. Unexpectedly, the positioning
103 of nucleosomes was not affected in *asf1* deletion strains. A significant reduction of DNA methylation
104 was observed in *S. macrospora* Δasf1, and a large number of genes that are usually weakly expressed
105 in wild type strains are upregulated in ∆asf1, indicating a role of ASF1 during gene regulation and DNA
106 methylation (18). The *S. macrospora* ASF1 has been shown to bind histones H3 and H4 (6), however, it
107 has not yet been analyzed if the histone-binding activity is actually required for fruiting body formation.
108 Therefore, in this study, we analyzed the histone binding function of ASF1 and its connection to sexual
109 development. We performed interaction studies and complementation analysis to verify the
110 importance of amino acid V94 (valine at position 94), a highly conserved histone interaction site known
111 from *in vitro* studies (7, 19). The C-terminal region of ASF1 is much less conserved than the first 155
112 amino acids and parts of it do not exist in animal or plant models (Figure 1). We generated truncated
113 versions of this region of *asf1* and used these to perform interaction studies and complementation
114 analysis to study the relevance of the divergent and functionally less well studied C-terminus of ASF1.
115 Additionally, we performed genomic stability assays based on growth under the influence of the
116 genotoxic substance methyl methansulfonate (MMS). We further focused on the role of ASF1 in
117 histone modification and chromatin structure by performing ChIP (chromatin immunoprecipitation)-
118 seq and Hi-C (chromosome conformation capture with high-throughput sequencing) experiments with
119 the wild type and the ∆asf1 mutant. For improved analysis of the ChIP-seq and Hi-C data, we first
120 generated a chromosome-level genome sequence of *S. macrospora*. Participation of ASF1 in histone
121 acetylation and deacetylation has been documented in *S. cerevisiae*, and a function during histone
122 methylation is regarded as highly probable and connections to the effect on DNA-methylation and
123 gene regulation might be possible (10). Therefore, ChIP-seq was performed for H3K27me3 and
124 H3K56ac. Furthermore, we performed Hi-C experiments to compare overall chromatin structure of
125 young, vegetative mycelium to older, sexual mycelium and *asf1* deletion mutants.
126
127

128

129 ## Materials and Methods

130

131 **Strains, crosses and growth conditions**

132 All strains used in this study have been summarized in Supplemental Table 1 and were cultivated on
133 either solid or liquid cornmeal medium (BMM) or complete medium (CM) at 25 °C as previously
134 described (20, 21). To perform genetic crosses, the spore color mutant fus was used as a partner to
135 allow the identification of recombinant asci (22). Transformation of *S. macrospora* was performed as
136 previously described (21).

137

138 **Cloning procedures, oligonucleotides and plasmids**

139 Plasmids encoding ASF1 variants with amino acid substitutions for complementation and interaction
140 analysis were generated by PCR mutagenesis and yeast recombinant cloning (23). Golden Gate cloning
141 was used to assemble plasmids encoding truncated ASF1 variants (24). Oligonucleotides for the
142 generation of plasmids and integration tests have been listed in Supplemental Table 2. All plasmids
143 used in this study are listed in Supplemental Table 3.

144

145 **Histone interaction assay by Co-Immunoprecipitation (Co-Ip)**

146 Plasmids coding for eGFP-tagged ASF1 variants were co-transformed together with plasmids encoding
147 FLAG-tagged histones H3 or H4 into the *S. macrospora* wild type strain SN1693 by protoplast
148 transformation (25). The resulting strains were grown for 4 d at 27 °C in 20 ml liquid BMM medium
149 with 50 µg / ml Nourseothricin. The mycelium was harvested by filtration and frozen in liquid nitrogen
150 before being ground into powder and mixed with protein extraction buffer (26). Co-
151 Immunoprecipitation was performed according to the manufacturers' instructions using GFP-Trap®
152 Beads (Chromotek) and ANTI-FLAG® M2 Beads (Sigma Aldrich). Raw and elution fractions were used
153 for SDS-PAGE (27) before being transferred to a PVDF membrane by western blotting. Co-Ip results
154 were generated with two biological replicates each for eGFP trapping and FLAG trapping. Signals for
155 eGFP and FLAG were detected by using Mouse Anti-GFP JL-8 (Clontech), Mouse Anti-Flag (Sigma
156 Aldrich) and Goat Anti-Mouse, HRP-linked (Cell Signaling) antibodies according to the manufacturers'
157 instructions.

158

159 **Complementation of *S. macrospora* with ASF1 variants and MMS tests**

160 Plasmids for the expression of ASF1 variants were generated from wild type genomic DNA with specific
161 primers amplifying *asf1* with specific substitutions or a shortened C-terminus and cloned by Golden
162 Gate Cloning (24) or via yeast homologous recombination (28). The *asf1* deletion strain SN1983 was

163 transformed with the respective plasmids by protoplast transformation resulting in ectopic integration
164 of the plasmid (25). Complementation strains that did not gain fertility on their own were crossed
165 against the wild type, and ascospores were isolated to obtain homokaryotic strains, while fertile
166 transformants were used to isolate ascospores directly (22). Phenotypical characterization was
167 performed by documenting the growth and fertility on BMM plates with a Stemi 2000-C
168 stereomicroscope (Zeiss). To evaluate the resistance against methyl methanesulfonate (MMS) all
169 strains were inoculated on BMM plates with 0.007 % MMS and growth was observed over a span of 7
170 d. The validity of the MMS assay was tested by checking the persistence of the effect of MMS on *asf1*
171 deletion mutants on 3 days old plates over a period of 7 days.
172
173 **Microscopic analysis**
174 For analysis of the subcellular localization of ASF1-EGFP fusion proteins, strains were grown on glass
175 slides together with strains expressing H3-MRFP fusion proteins as described (29). Light and
176 fluorescence microscopy was performed with an AxioImager microscope (Zeiss, Jena, Germany) with
177 a Photometrix Cool SnapHQ camera (Roper Scientific). EGFP fluorescence was detected with Chroma
178 (Bellows Falls, VT, USA) filter set 41017 (HQ470/40, HQ525/50, Q495lp) and mRFP fluorescence was
179 detected with set 49008 (EG560/40x, ET630/75 m, T585lp). Images were further handled by using
180 MetaMorph (Molecular Devices).
181
182 **Extraction and sequencing of genomic DNA from *S. macrospora***
183 For DNA preparation for nanopore sequencing, the wild type strain SN1693 was grown for 2 d at 27 °C
184 in 20 ml liquid CM medium (25) in petri dishes, harvested by filtration and ground in liquid nitrogen.
185 500 µg of ground mycelium was used for extraction of high molecular weight DNA with the NucleoBond
186 HMW-Kit (Macherey-Nagel, Düren, Germany) according to the manufacturer's instructions. A
187 sequencing library with wild type genomic DNA was prepared using the Nanopore DNA Ligation
188 Sequencing Kit (SQK-LSK109, Oxford Nanopore Technologies, Oxford, UK) according to the
189 manufacturer’s instructions. Sequencing was performed on an Oxford Nanopore GridION Mk1
190 sequencer using an R9.4.1 flow cell, which was prepared according to the manufacturer’s instructions.
191 Basecalling was performed using guppy v5.0.11 with the super-accurate basecalling model. A total of
192 290927 reads were obtained with an average read length of 15874 bp and an N50 of 23018 bp.
193 For DNA preparation for Illumina sequencing of the Δasf1 mutant, the Δasf1 strain SN1983 was grown
194 for 3 d at 27 °C in 20 ml liquid CM medium in petri dishes, harvested by filtration and ground in liquid
195 nitrogen. DNA preparation was performed as described previously for *Pyronema confluens* (30). Library
196 preparation and Illumina sequencing of a 300 bp insert library (150 bp paired-end sequencing) were
197 performed at Novogene (Cambridge, UK).

198

199 **Genome assembly and annotation**

200 Nanopore reads were assembled with SMARTdenovo (available at
201 https://github.com/ruanjue/smartdenovo, accessed on 2021/06/29) resulting in nine contigs with a
202 total size of 39.4 Mb. The initial assembly was subjected to four rounds of correction with Racon (31)
203 using the nanopore reads for correction, and subsequently three rounds of correction with pilon
204 (v1.24) (32) based on previously generated *S. macrospora* genomic Illumina reads (33) (NCBI SRA
205 database, accession number SRR5749461). BLAST comparisons (34) with a previously generated *S.*
206 *macrospora* genome assembly (35) showed that the smallest contig (161 kb) most likely contained
207 mitochondrial DNA. This contig was removed, and the remaining eight contigs were analyzed for
208 putative telomeric repeats (sequence TTAGGG) using a custom-made perl program. Telomeric repeats
209 were found at both ends of five contigs, and at one end each in the remaining three contigs. Of the
210 latter, one contig contained the rDNA repeats at the end without telomeric repeats. The other two
211 non-telomeric contig ends were compared to each other and found to have an overlap of 2.2 kb with
212 100 % sequence identity, making it likely that these contigs were part of the same chromosome. The
213 contigs were fused manually, and the junction was checked for continuity by mapping the nanopore
214 reads to the assembly with graphmap (36). The resulting assembly consists of 7 contigs with a total
215 size of 39.4 Mb and an N50 of 5.7 Mb. Comparison to the genome assembly of the closely related
216 ascomycete *Neurospora crassa* (FungiDB version 52) (37, 38) was performed with nucmer from the
217 MUMmer package (v4.0.0rc1) (39).

218 Genome annotation of protein-coding genes was performed with MAKER (v3.01.03) (40) based on
219 transcripts and proteins from a previous annotation of the *S. macrospora* genome (33) as well as on
220 the *N. crassa* proteins (38) from FungiDB version 52 (37). tRNAs were annotated with tRNAscan-SE
221 (v2.0.8) (41). rDNA repeats were annotated manually based on BLAST comparisons. *S. macrospora*
222 locus tags from a previous annotation (33) were mapped onto the predicted gene models based on
223 BLAST results. Approximately 1200 gene models were manually corrected in the genome browser
224 Artemis (42) based on RNA-Seq data generated previously (18, 43) (NCBI GEO accession numbers
225 GSE33668 and GSE92337) that were mapped to the assembly with Hisat2 (v2.2.1) (44).

226

227 **Western blot analysis of histone modifications and chromatin immunoprecipitation**

228 Potential targets for ChIP-seq experiments were selected based on semiquantitative western blot
229 screenings with antibodies against histone modifications previously suspected to be influenced by
230 ASF1. The wild type strain SN1693, the Δasf1 strain SN1983, and complementation strains expressing
231 *asf1* variants with amino acid substitutions or a truncated C-terminal region, were cultivated in liquid
232 CM medium (25) for 3d and 4d, respectively, at 27 °C, harvested by filtration and washed with an

233 isotonic buffer established for protoplasts (PPP) (21). Samples were frozen in liquid nitrogen and
234 ground into a fine powder. Proteins were extracted by mixing the powder with extraction buffer (50
235 mM Tris/HCl pH 7.5, 250 mM NaCl, 0.05 % NP-40, 0.05 % β-mercaptoethanol, 0,3 % (v / v) Protease
236 Inhibitor Cocktail Set IV (Calbiochem)) and 20 min centrifugation. Protein concentrations were
237 determined by Bradford assays (45) and equal amounts were loaded and separated by SDS
238 gelelectrophoresis and transferred to a PVDF membrane by western blotting. Antibodies against target
239 histone modifications were used to detect respective bands (Anti H3K27Me3 #9733 Cell Signaling, Anti
240 H3K9Me #ABE101 Merck Millipore, Anti H3K56Ac #61061 Active Motif, Anti H3K9Ac #39038 Active
241 Motif, Anti H3 #9715 Cell Signaling), detection protocols have been summarized in Supplemental Table
242 4. Band strengths were compared by using a ChemiDoc XRS+ system (BioRad) with Image Lab 4.0
243 software (BioRad). Normalization for the total amounts of protein in the samples was based on
244 Coomassie-stained gels run in parallel. The level of histone H3 was assessed as an internal control.
245 Modifications that exhibited significant differences between wild type and deletion mutant were
246 selected for ChIP-seq experiments. ChIP-samples were cultivated similar to the samples for western
247 blotting and crosslinking was performed in PPP buffer with 1% formaldehyde for 15 min at room
248 temperature, followed by a quenching time of 15 min by an excess amount of glycine. After three PPP
249 washing steps, lysis was conducted in extraction buffer (50 mM Tris/HCl pH 7.5, 250 mM NaCl, 0.05 %
250 NP-40, 0.05 % β-mercaptoethanol, 0,3 % (v/v) Protease Inhibitor Cocktail Set IV (Calbiochem)) for 15
251 min on ice by frequent vortexing. After centrifugation, chromatin solution was obtained and mixed
252 with MNase buffer (18) and proteinase inhibitors. Chromatin digestion was conducted by incubation
253 with 200 U/ml MNase (Thermo Fisher Scientific) for 105 min at 37 °C under constant shaking and
254 stopped by adding EDTA to a concentration of 20 mM. Aliquots were removed as input samples, and
255 immunoprecipitation performed over night at 4 °C on a spinning wheel by adding 10 µl of the
256 respective antibody (Anti H3K27Me3 #9733 Cell Signaling, Anti H3 #2650 Cell Signaling, Anti H3K56Ac
257 #61061 Active Motif). Afterwards, 4 h of incubation on Protein-A agarose beads (Santa Cruz) were
258 followed by 2 washing steps in low salt (50 mM Tris-HCL pH 7.5, 10 mM EDTA, 10 mM NaCl) and 2
259 washing steps in high salt buffer (50 mM Tris-HCL pH 7.5, 10 mM EDTA, 500 mM NaCl). Each washing
260 step was performed for 5 min at 4 °C on a spinning wheel and followed by 2 min of centrifugation at
261 2500 rpm to separate the beads from the buffer (46). Chromatin was washed off the beads by 2 h of
262 incubation in TE buffer with 1 % SDS at 65 °C and de-crosslinked over night at 65 °C after adding 2
263 mg/ml Proteinase K (Genaxxon bioscience). Standard phenol/chloroform extraction was performed to
264 isolate DNA from the ChIP and input samples. Two biological replicates each were created for H3,
265 H3K27me3 and H3K56ac. Fragment sizes were evaluated on a Bioanalyzer 2100 (Agilent) according to
266 the requirements for ChIP-seq samples set by Novogene. Samples that contained at least 20 ng of
267 fragments in the range of 150 to 500 bp were selected and further processed. Size selection for

268 fragments between 150 and 500 bp and library generation was performed at Novogene (Cambridge,
269 UK) , as well as Illumina sequencing (150 bp paired-end) of ChIP and input samples. The detailed ChIP-
270 seq protocol can be found in Supplemental Text 1.
271
272 **ChIP-seq peak detection**
273 At least 30 million paired-end reads per sample were sequenced at Novogene (Cambridge, UK). The
274 obtained reads were trimmed with fastp 0.23.2 (47) and mapped to the reference genome of *S.*
275 *macrospora* SN1693 by using BWA-MEM 0.7.17 with default parameters (48). Deduplication and input
276 corrected peak detection were performed for the samples of H3, which were subsequently used
277 together with the native input samples as control for H3K27me3 and H3K56ac by using MACS2 callpeak
278 2.2.7.1 in paired end mode. For both histone marks, broad regions were identified with a 0.01
279 minimum FDR (false discovery rate) cutoff and an effective genome size of 39 Mb (49, 50). Differential
280 peak analysis was conducted by discarding overlapping peaks in wildtype and Δasf1 using BEDTools
281 2.30.0 with a minimum overlap of 10 % (51). Peaks were annotated to the reference genome using
282 HOMER annotatePeaks 4.9.1 (52).
283
284 **Hi-C sample preparation**
285 Young wild type samples of SN1693 where cultivated for 2 d at 27 °C in liquid CM medium (25). Samples
286 for the older wild type were grown for 5 d and Δasf1 SN1983 for 3 d under the same conditions.
287 Mycelium was harvested by filtration, washed with PPP (21) and frozen in liquid nitrogen. The Omni-C
288 library was prepared using the Dovetail® Omni-C® Kit according to the manufacturer's protocol with
289 additional changes to enable the use on *S. macrospora*. Briefly, the chromatin was fixed with 1 %
290 formaldehyde for 10 min at room temperature on a spinning wheel and quenched by bringing the
291 solution up to 200 mM glycine. The cross-linked chromatin was then digested in situ with DNase I
292 according to the manufacturer's instructions. Following digestion, the cells were lysed in 1 % SDS to
293 extract the chromatin fragments and the chromatin fragments were bound to Chromatin Capture
294 Beads. Next, the chromatin ends were repaired and ligated to a biotinylated bridge adapter followed
295 by proximity ligation of adapter-containing ends by using the reagents supplied by the Dovetail® Omni-
296 C® Kit. After proximity ligation, the crosslinks were reversed at 68 °C in Dovetail® Crosslink Reversal
297 Buffer and 1 µg / µl Proteinase K overnight. The DNA was purified with SPRIselect™ Beads (Beckmann
298 Coulter) and 150 ng were converted into a sequencing library using Illumina-compatible adaptors by
299 using the Dovetail® Library Module for Illumina®. Biotin-containing fragments were isolated using
300 streptavidin beads prior to PCR amplification. Illumina sequencing (150 bp paired-end) was performed
301 by Novogene (Cambridge, UK).
302

303 **Generation of Hi-C maps**

304 Hi-C maps were created by following the Dovetail® Omni-C® Pipeline with adjustments for the genome
305 of *S. macrospora*. Reads were trimmed with fastp 0.23.2 (47) and mapped to the reference genome of
306 *S. macrospora* SN1693 by using BWA-MEM 0.7.17 with default parameters (48). Valid ligation events
307 were recorded by using pairtools 1.02 (53) parse with a min-map quality of 40 and a max-inter-align-
308 gap of 30 before being sorted by pairtools sort. PCR duplicates were removed by using pairtools dedup
309 and the pairs file was generated by pairtools split. The hic matrix was generated by using juicertools
310 1.6.2 (54) with standard parameters.

311

312 **Data availability**

313 Nanopore reads and the chromosome-resolved genome sequence for the *S. macrospora* wild type
314 strain SN1693 were deposited in the NCBI databases under BioProject ID PRJNA744349
315 (http://www.ncbi.nlm.nih.gov/bioproject/744349, SRA accession number SRR15901728 for the
316 nanopore reads, DDBJ/ENA/GenBank accession numbers CP083903-CP083909 for the seven
317 chromosomes). ChIP-seq and Hi-C data generated in this study were submitted to the NCBI GEO
318 database as a superseries under accession number GSE216634
319 (https://www.ncbi.nlm.nih.gov/geo/query/acc.cgi?acc=GSE216634, accession numbers GSE216629
320 and GSE228529 for ChIP-seq data and GSE216632 for Hi-C data). Illumina reads from the Δasf1 strain
321 were deposited in the NCBI SRA database under BioProject ID PRJNA922040
322 (https://www.ncbi.nlm.nih.gov/sra/PRJNA922040).

323

324

325 **Results**

326

327 **A chromosome-level genome assembly of *S. macrospora***

328 The nuclear genome of *S. macrospora* was previously shown by pulsed-field gel electrophoresis to
329 consist of seven chromosomes (21). Prior to our study, three genome assemblies of *S. macrospora*
330 have been generated with increasing continuity (33, 35, 55); however, even the latest genome
331 assembly still consists of 584 scaffolds (33) and would therefore be unsuited for analyses at
332 chromosome level. Therefore, to aid in the planned Hi-C and ChIP-seq analyses, we generated a
333 chromosome-level genome assembly of *S. macrospora* based on nanopore sequence reads. The new
334 assembly (*S. macrospora* genome version 04) consists of seven gapless contigs with a total size of 39.4
335 Mb (Figure S1) which is similar in size to previous assemblies and to estimates by pulsed-field gel
336 electrophoresis of 39.5 Mb (21, 33, 35, 55). Six of the seven contigs have telomeric repeats at both
337 ends, whereas one contig has telomeric repeats at one end and 10 copies of the ribosomal RNA (rRNA)

genes at the other end with the repetitive nature of the rRNA genes most likely preventing assembly of telomeric repeats at that end. This indicates that the seven contigs represent the seven chromosomes of *S. macrospora*. A comparison with the genome assembly of the closely related ascomycete *Neurospora crassa* showed a high degree of synteny for the seven chromosomes of each species, consistent with previous analyses of smaller genomic regions of the two fungi (35, 56) (Figure S1). Thus, a chromosome-level assembly for *S. macrospora* is now available and can be used for analyses at chromosome level.

S. macrospora ASF1 depends on V94 and large parts of the C-terminus to accomplish histone binding

The function and structure of ASF1 is highly conserved in all eukaryotes and it has been described as a central histone chaperone that binds the histones H3 and H4 as a dimer and individually. The first 155 amino acids form a globular core in which acidic patches allow for the interaction with both histones (7). Especially the area surrounding position V94 has been shown to be essential for ASF1-histone binding in yeast (19). However, little is known about the functions of the C-terminal tail. This region is much more divergent than the globular core and parts of it exist in fungi, but not in animals or plants, with the region after amino acid 210 being restricted to ascomycetes (Figure 1). To analyze if V94 is required for histone binding of *S. macrospora* ASF1, we performed co-immunoprecipitation experiments with an ASF1 variant that includes a V94R substitution and a variant with a D37A substitution. The latter is a mutation of an interaction site with the histone chaperone HIRA that was identified in *S. pombe* (57). In addition, ASF1 variants with truncations after positions 152, 185 and 210 were generated to gain insight into possible involvement of the C-terminal region in the process of histone binding. In GFP- and FLAG-trap experiments, the V94R variant proved to be incapable of pulling down the histones H3 and H4, while the D37A variant performed like the wild type ASF1 (Figure 2, Supplemental Figures 2 and 3). Thus, the conserved V94 is required for histone interactions in *S. macrospora*, whereas the putative HIRA interaction site D37 is not. Truncated ASF1 variants were also unable to bind H3 and H4 when the truncations occurred after positions 152 or 185. Truncation after position 210 had no detectable effect and did not impair the capability to pull down the histones (Figure 3, Supplemental Figures 4 and 5).

The histone binding function of ASF1 is essential for sexual development

We used the *asf1* variants described above carrying substitutions in the histone binding site V94, the putative HIRA interaction site D37 and variants with truncated C-terminal regions for complementation analysis in a previously constructed *asf1* deletion strain (6). By correlating the ability of these variants for rescuing the phenotype of the deletion mutant with information about their ability to bind histones, more insights into the role of ASF1-histone interaction during multicellular development can

373 be gained. The *asf1* deletion mutant was transformed with plasmids coding for the respective variants,
374 and homokaryotic strains were obtained by the isolation of ascospores from self-fertile perithecia or
375 from genetic crosses. PCR screenings confirmed the integration of *asf1* variants in the resulting
376 transformants (Supplemental Figure 6). The phenotype of the resulting strains was documented after
377 growth for a week on BMM medium. *S. macrospora* Δasf1 is sterile and mostly consists only of
378 vegetative mycelium, but is sometimes able to generate small protoperithecia. Introducing the wild
379 type *asf1* gene back into the deletion mutant led to a complete reversal of the deletion phenotype and
380 yielded strains indistinguishable from the wild type, gaining full fertility. Strains expressing the D37A
381 variant also regained fertility, but showed slightly reduced complementation rates (Table 1). These
382 strains were able to form perithecia, but exhibited slight aberrations with a tendency to grow aberrant
383 perithecia and giant protoperithecia (Supplemental Figure 7). A reintroduction of an ASF1 variant with
384 a V94R substitution did not complement the deletion mutant and the resulting strains exhibited the
385 same phenotype as Δasf1 strains (Figure 4, Table 1). Since ASF1 V94R does not complement the sterile
386 phenotype of deletion mutants and is unable to bind histones, a connection between histone binding
387 and sexual development seems likely. ASF1 D37A proved to have no disruption in histone binding and
388 regained fertility, but the substitution in a putative HIRA-binding site still had impact on the life cycle
389 of *S. macrospora*, as evident by the formation of some aberrant perithecia. However, histone binding
390 capability was enough to reach fertility. Truncations of ASF1 at positions 152 and 185 led to strains
391 that resembled the deletion mutant, but a truncation at position 210 still allowed for full
392 complementation (Figure 4, Table 1). Thus, although the C-terminal tail of ASF1 is less conserved, parts
393 of it are essential for histone binding and sexual development. Leaving only the core intact or
394 shortening the protein to 185 amino acids seems to have the same effect on both processes as a full
395 deletion. A truncation after position 210 removes the part of ASF1 that is only present in ascomycete
396 fungi and does not affect its overall functionality. To rule out the possibility of protein mislocalization
397 as a cause for the inability to complement the deletion mutant, the eGFP-tagged variants were tracked
398 by fluorescence microscopy. All of them co-localized with an mRFP-tagged H3 in the nucleus
399 (Supplemental Figure 8), similar to what was previously shown for wild type ASF1 (6).
400

401 **ASF1 can contribute to DNA damage protection even without histone binding capabilities**

402 Even after confirming the correct localization of tested ASF1 variants, a possible complete loss of
403 function of the protein, i.e. not specifically related to histone binding, could not be completely ruled
404 out. Thus, we looked for a way to confirm functionality of the variants aside from histone binding *in*
405 *vivo*. The complex network of ASF1 regarding chromatin modification is still poorly understood and
406 direct functions beyond nucleosome assembly are not widely known. It was previously shown in *S.*
407 *cerevisiae* that ASF1 is involved in DNA damage protection, since Δasf1 mutants are unable to grow on

408 the DNA damage-inducing agent MMS (58). However, in *S. cerevisiae* C-terminal truncations had no
409 impact on DNA damage protection abilities of ASF1 (59, 60). Therefore, we tested *S. macrospora* Δasf1
410 and the strains expressing the variants for their reaction to the DNA damaging agent MMS, which
411 causes DNA single- and double strand breaks. At a concentration of 0.007 % MMS (v/v), the wild type
412 was able to grow normally on BMM medium, while the mutant did not grow at all (Figure 5).
413 Complementation strains expressing ASF1 variants D37A and 210T showed wild type-like resistance.
414 Although the V94R, 152T and 185T variants of ASF1 are indistinguishable from the deletion strain
415 under normal conditions, an increased resistance against MMS compared to the ∆asf1 strain was
416 clearly visible (Figure 5).
417 Since MMS is known to be a highly reactive chemical and could be inactivated in the media after a
418 short time, we performed a persistence test for our plates. MMS plates were inoculated with the
419 sensitive Δasf1 strain two days after their production and growth was observed for 7 days
420 (Supplementary Figure 9). After the plates reached an age of 7 days, weak growth of the sensitive
421 strain was observed. After this time, Δasf1 appeared to be able to grow on the MMS plates. Therefore,
422 we conclude that although 0.007% MMS plates are volatile and cannot be used for a long time, but
423 during our observation period of 4 days on freshly prepared plates, MMS can be used to assess the
424 resistance of *S. macrospora* to genotoxic stress.
425 The difference between *S. macrospora* strains expressing these ASF1 variants and the deletion mutant
426 suggests that an uncharacterized function of ASF1 in DNA damage protection exists and these variants
427 are functional in this regard even though some of them are not able to bind histones. Thus, the data
428 suggest that the role of ASF1 in DNA damage protection does not depend on histone interaction.
429
430 **Deletion of *asf1* changes global histone modification levels in *S. macrospora***
431 The functions of ASF1 as a central histone chaperone and its multiple interaction partners during
432 chromatin modification suggest a participation in processes like histone modification. Indeed, ASF1
433 has been shown to be involved in the acetylation of H3 on the lysines 9 and 56 in *S. cerevisiae* (9) and
434 changes in the deposition of H3K27me3 and H3K9me3 have been observed in *M. musculus* cells during
435 ASF1 depletion conditions (10). To gain insight into the role of ASF1 in histone modification, we
436 performed semi-quantitative western blot screens with protein extracts from *S. macrospora* wild type
437 and Δasf1 for histone modifications H3K27me3, H3K9me, H3K56ac, and H3K9ac. The comparison of
438 the band strength after incubation with antibodies specific for these modifications indicated significant
439 changes in global histone modification levels for H3K27me3 and H3K56ac in the ∆asf1 mutant (Figure
440 6). To gain further insight into the relevance of histone binding for the establishment of histone
441 modifications in ASF1 affected pathways, we also performed semiquantitative screens for ASF1
442 variants with amino acid substitutions and a truncated C-terminal tail (Figure 6). Our observations

443 mimic our results for complementation capacity and histone binding, as variants that were unable to
444 restore the wild type phenotype and bind histones also showed alterations in H3K27me3 and H3K56ac
445 that were comparable to the deletion mutant. Because of the clear effect of an *asf1* deletion on
446 H3K27me3 and H3K56ac levels, we chose these histone modifications as candidates for ChIP-Seq
447 experiments to verify the results of the screening and to gain information about the distribution of
448 both histone marks. Establishing this method for older mycelium of *S. macrospora* presented
449 challenges regarding the crosslinking and shearing process, as crosslinking agents appeared to create
450 an agglomeration of inaccessible cells. A combination of high input amounts, soft lysis conditions and
451 DNase based shearing allowed us to conduct reproducible ChIP-seq experiments on older
452 *S. macrospora* samples for the first time (Supplemental Text 1, Supplemental Figure 11). All sequenced
453 samples resulted in more than 30 million paired-end reads that showed minimal sequence- or mapping
454 based duplication rates after mapping to the reference genome (Supplemental Figure 12). Duplicates
455 were discarded by MACS2 and broad peak detection was performed for both histone marks (50). The
456 fraction of reads in peaks surpassed the 0.01 threshold (Supplemental Table 5) determined by the
457 ENCODE project for successful ChIP-seq experiments for all samples (61). Repeatability was assessed
458 by Pearson and Spearman correlation and a positive correlation was detected for our replicates
459 (Supplemental Figures 13 and 14). Consistent with the results of Western blot analysis, ChIP-seq
460 revealed that the number of unique ChIP peaks as well as the number of transcriptional start sites and
461 their surrounding 2 kb regions exhibiting H3K27me3 was increased in the deletion mutant whereas
462 H3K56ac appeared to be strongly decreased (Figure 7A, Supplemental Table 6). Although global levels
463 of these histone marks were visibly affected by the deletion of *asf1*, the increase or decrease did not
464 lead to a significant shift of positioning of these marks with regards to the deposition at exons, introns,
465 TSS, TTS or intergenic regions when observed on a relative level (Figure 7B). Therefore, the changes in
466 histone modification strength seem to be more general and not restricted to exons or other functional
467 genomic regions. Representative peaks for exonic regions are shown in Figure 7C, additional
468 representative regions are presented in Supplemental Figure 15.
469

470 **Hi-C reveals a 600 kb duplication in *asf1* deletion mutants that might be linked to their survival**

471 To study the effect of *asf1* and sexual development on overall chromatin structure, we performed Hi-
472 C experiments to map the abundance of DNA-DNA interactions in mycelium at two different
473 developmental stages of the wild type and in mycelium of Δasf1. Samples for the young wild type were
474 grown for 2 d, thus most of the mycelium consisted of vegetative tissue and sexual development was
475 in its early stages. Samples for older mycelium were grown for 5 d, at this stage fully melanized
476 protoperithecia and some early perithecia can be expected. The deletion mutant was cultivated for 3
477 d (since it is growing somewhat slower than the wild type), but is blocked in its sexual development at

478 the stage of very young protoperithecia. The chromatin of the samples was fixed with formaldehyde
479 and treated with DNase to obtain crosslinked pairs of DNA that are in close proximity at that time. Ends
480 were filled with biotin and re-ligation was performed under high dilution conditions, so ligation events
481 of crosslinked strands are more likely. A streptavidin pulldown was used to generate samples
482 containing interacting DNA fragments of a sample at the given time. By using Dovetail® Dual index
483 primers, Illumina® libraries of around 50 ng were obtained and used for high throughput paired end
484 sequencing. Almost all samples generated over 50 million paired end reads that were mapped to the
485 reference genome and used for the generation of Hi-C maps. Hi-C contacts appeared to be quite low,
486 averaging around 11 %, indicating low complexity (Supplemental Table 7). All recorded interaction
487 events were plotted against their position on the *S. macrospora* genome, each one represented by a
488 red dot. The intensity of red dots at a specific area indicates more recorded DNA-DNA interactions in
489 the sample at the tested point in time. The characteristic diagonal line is an indicator of the high
490 interaction frequency of genomic regions that are always in close proximity to each other, because of
491 their vicinity on the DNA strand itself (Figure 8A). While the resolution of the generated Hi-C maps
492 was too low to make out specific compartments of the young and old wild type, a significant reduction
493 of the general resolution in the sexual mycelium might hint at the development of multiple cell types
494 with different chromatin conformations. During sexual development *S. macrospora* generates multiple
495 different cell types (4), therefore it seems likely that different cell types are characterized by different
496 chromatin conformations. The presence of more than one chromatin conformation in a sample could
497 lead to a loss of signal for mappable DNA-DNA interactions at a specific point.
498 The Hi-C map of the deletion mutant appeared to show a strong increase of DNA-DNA interactions of
499 a specific region of 600 kb on chromosome 2 with all other genomic regions (enhanced horizontal and
500 vertical bars in Figure 8A). However, such an explanation is biologically unlikely, and a more likely
501 explanation would be that this genomic region in the ∆asf1 mutant differs from the wild type genome
502 that was used as a reference for mapping. In this case, this strong increase hinted at a duplication of
503 this region in Δasf1, which would result in twice the number of reads, which then all mapped to the
504 single copy of the wild type genome that was used as a reference for the generation of the Hi-C map.
505 This would also lead to twice the number of (spurious) interactions with other regions of the genome,
506 which would appear as the observed enhanced horizontal and vertical bars in the Hi-C contact map.
507 We detected read patterns in the Hi-C data that match the internal border of a putative tandem
508 duplication of the area of interest. To test this, we sequenced the genome of the ∆asf1 mutant by
509 Illumina sequencing. Sequencing reads were mapped to the wild type reference genome, which proved
510 the existence of the duplication in the deletion mutant (Figure 8B, Supplemental Table 8). The detected
511 duplication consists of two compartments, with the middle region of the area of interest not
512 duplicated, hinting at a loss event or two independent duplication events.

513 PCR tests with primers amplifying the newly created internal junctions of the duplicated area (Figure
514 8C) revealed the existence of the duplication in all used ∆asf1 strains even those that resulted from
515 backcrosses against the wild type. Since the *asf1* gene is located on chromosome 6, whereas the
516 duplication is present on chromosome 2, they should segregate independently resulting in
517 approximately 50 % of ∆asf1 strains with and 50 % without the duplication in a cross with a wild type
518 strain. Therefore, we suspected that the viability of the *asf1* deletion might depend on the presence
519 of the duplication. Crossing experiments were performed to analyze the correlation between viable
520 Δasf1 strains and the duplication. The crosses with the spore color mutant fus, which carries the wild
521 type *asf1* allele, resulted 69 strains with an *asf1* wild type allele, of which 21 contained the duplication,
522 matching expectations for free recombination. The 42 ∆asf1 mutant strains all possessed the
523 duplication, suggesting that the viability of ∆asf1 strains is indeed linked to the occurrence of the
524 duplication on chromosome 2 (Table 2, Supplemental Table 9). While screening for duplication-free
525 Δasf1 strains, we also screened strains carrying *asf1* variants with amino acid substitutions that we
526 used in the complementation analysis, and found the absence of the duplication in several strains
527 containing ASF1 variants V94R, D37A, 185T and 152T (Table 2, Supplemental Table 9). While the
528 absence of the duplication in D37A strains is not surprising since they are fertile and able to interact
529 with histones, the V94R, 185T and 152T variants are unable to bind histones and do not complement
530 the developmental phenotype of *asf1* deletions. This suggests that the presence of an ASF1 protein
531 even without histone binding ability is sufficient to overcome the potential lethality of the complete
532 absence of ASF1, whereas the complementation studies described above show that ASF1 without
533 histone binding ability is not sufficient for fruiting body development. The presence of the duplication
534 does not appear to have any additional effect on the strains carrying it, since all strains show the same
535 phenotype whether the duplication is present or not (fertile for wild type and D37A, sterile for V94R,
536 185T and 152T, Supplemental Table 9).
537
538 **Discussion**
539
540 ***S. macrospora* ASF1 needs an intact C-terminal region to perform histone binding, an essential**
541 **function for sexual development**
542 Next to *A. thaliana* (17), *S. macrospora* is one of only two known multicellular organisms that survive
543 a full deletion of *asf1* (even though this appears to be contingent on the presence of the duplication
544 on chromosome 2 as described above), making it a valuable model for ASF1 *in vivo* research, especially
545 when its fast vegetative growth and sexual cycle are taken in account. Therefore, we have the unique
546 opportunity to study the importance of *asf1* for multicellular development. *asf1* deletion strains have

547 been shown to exhibit a slowed vegetative growth rate, and sexual development is blocked at the
548 stage of young protoperithecia (6).
549 The ability to interact with histones can be regarded as the central requirement of a histone chaperone
550 to perform its functions. ASF1 is known to interact with the histones H3 and H4 and deposits them
551 during nucleosome assembly during transcription, replication and DNA-repair. The general interaction
552 mode of ASF1 with H3 and H4 has been analyzed by *in vitro* experiments with *S. cerevisiae* proteins.
553 The central acidic patch in the core of ASF1 and especially the amino acid V94 are essential in this
554 regard (7). Since the first 155 amino acids of ASF1 are highly conserved in all eukaryotes, similar
555 functions can be assumed. In fact, our co-immunoprecipitation experiments showed a clear
556 dependency of *S. macrospora* ASF1 on V94 to establish interactions with H3 and H4. However, the C-
557 terminal region of ASF1 is quite divergent, with some parts existing in fungi but not in animal or plant
558 models, so information about the functional relevance of this region is sparse. Although experiments
559 in *S. cerevisiae* showed a contribution of the C-terminal region of ASF1 to histone interaction and gene
560 silencing, the specific interaction mode still remains elusive (59). Since the unicellular nature of yeasts
561 does not allow for the analysis of multicellular developmental processes and the specific region of ASF1
562 is quite divergent, experiments in multicellular eukaryotes like *S. macrospora* might shed more light
563 on the functions of this part of ASF1. Co-immunoprecipitation showed that despite of this region's
564 divergent nature it is essential for establishing a connection between ASF1 and H3-H4 up until amino
565 acid 210. Thus, a function of the C-terminal tail during this interaction is highly likely. The acidic nature
566 of the C-terminal tail might contribute to facilitating the connection between ASF1 and the histones.
567 A physical interaction between the C-terminal region and H3-H4 has not yet been detected, but might
568 be difficult to prove with structural analysis, because of the usually unfolded C-terminus (58). ASF1 is
569 known to bind histones H3 and H4, but prior to this study, it was not clear if histone binding is required
570 for sexual development. We therefore analyzed different ASF1 variants for their ability to bind histones
571 as well as their ability to support fruiting body formation. Since all ASF1 variants that did not co-
572 immunoprecipitate the histones H3 and H4 were unable to restore the deletion phenotype, the histone
573 binding function of ASF1 appears to be fundamental for sexual and therefore complex multicellular
574 development. Complementation experiments with ASF1 variants that were shown to be able to bind
575 histones led to fully fertile strains, underscoring the importance of this function for normal
576 development. With the exception of ASF1 D37A, these variants generated *S. macrospora* strains that
577 resembled the wild type. D37A strains exhibited a light brown coloration of the mycelium and a
578 tendency to generate aberrant perithecia that resembled giant protoperithecia and exhibited a slightly
579 reduced fertility. Since D37 is the putative interaction site of ASF1 with the histone chaperone complex
580 HIRA (19), one might speculate about an involvement of HIRA during melanin biosynthesis and sexual
581 development.

582

583 **Histone binding is not essential for the function of ASF1 during DNA-damage repair**

584 A role of ASF1 during DNA-damage repair without usage of its histone chaperone activity has often
585 been suspected and indeed, in recent studies with human ASF1A, a connection to double strand repair
586 mechanisms independent of histone binding has been discovered (62). In *S. macrospora*, strains
587 expressing ASF1 variants defective in histone binding were able to survive genotoxic stress, whereas
588 Δasf1 proved to be highly sensitive. It can therefore be concluded that the constructed ASF1 variants
589 are at least partially functional in DNA damage repair and that the observed defects in fruiting body
590 development are specifically related to the ability to perform canonical histone chaperone functions.
591 One hypothesis might be that ASF1 is not only a histone chaperone, but also functions as a chromatin
592 modifier hub that regulates and supports the activity of other chromatin-modifying proteins.
593 Regarding the involvement in DNA damage repair, multiple interaction partner candidates are
594 conceivable. A histone-independent interaction with RIF1 has already been demonstrated in human
595 cell lines and contributes to determining the choice of the appropriate double strand break repair
596 mechanism (62). Another candidate involved in DNA damage protection and possibly activated by ASF1
597 is the histone acetyltransferase RTT109. RTT109 is responsible for H3K9 and K56 acetylation,
598 modifications that are known to be important for DNA damage resistance (63). Interaction between
599 ASF1 and RTT109 has been characterized for *S. cerevisiae* (9) and an activating effect on the histone
600 acetyltransferase was shown, although the exact mechanism remains elusive (64). A defect in
601 acetylation of H3 in *asf1* deletion mutants has been also demonstrated in our ChIP-Seq experiments,
602 therefore a connection between the increased sensitivity of *S. macrospora* Δasf1 to DNA damage and
603 lowered activity of RTT109 seems possible, but the results from H3K56ac screenings for histone-
604 binding defective *asf1*-variants demonstrate that this effect cannot be solely responsible for the
605 increased sensitivity of Δasf1 strains to DNA damage. Strains expressing variants unable to interact
606 with histones, as shown in our interaction study, showed resistance in the DNA damage assay, even
607 though the reduction in H3K56ac was highly similar to the deletion mutant. A combination of multiple
608 factors therefore appears likely. Reduction of H3K56ac might a contributing factor to the MMS
609 sensitivity of the mutant, but additional ASF1-dependent factors might be defective without this
610 central histone chaperone.

611 Another ASF1-mediated factor for DNA stability is known in *S. cerevisiae* as the checkpoint kinase
612 RAD53 and is involved in DNA-double strand break repair mechanisms. RAD53 needs to be inactivated
613 and bound to ASF1 after repair has been completed, and lack of ASF1 could lead to an overabundance
614 of active RAD53 and subsequent disturbances in the cell cycle and further damage repairs (65). All in
615 all, ASF1 seems to play a crucial role during multiple DNA-damage protection and repair pathways, not
616 all of them relying on ASF1-H3/H4 interactions.

617

618 **ASF1 is involved in the histone modification landscape of *S. macrospora***

619 The histones are targets of various posttranslational modifications. The best known are acetylation,
620 methylation, phosphorylation, sumoylation, and ubiquitination. These modifications vary throughout
621 the genome and shape the histone code, which in turn influences access to the DNA for transcription
622 and the recruiting of transcription factors. The histone landscape of a cell is a significant determinant
623 of the transcriptome (66). ASF1 as a central eukaryotic histone chaperone has been reported to affect
624 multiple histone modifications, such as acetylation of H3K56 (9) and methylation of H3K27 (10). These
625 modifications undergo significant changes after deletion of *asf1* in *S. macrospora*. For H3K27me3, a
626 well-known heterochromatin modification (67), the *asf1* deletion mutant showed 1142 unique ChIP
627 peaks compared to only 401 unique peaks in the wild type. The increase in unique H3K27me3 positions
628 did not seem to be site-specific, as the relative distribution was comparable in the mutant and the wild
629 type. In general, we did not observe a significant change of H3K27me3 in specific functional regions,
630 like transcriptional start sites or gene bodies, instead the global level of this modification was affected
631 as a whole. The increase of H3K27me3 in *asf1* deletion strains could either be a direct consequence of
632 a disruption of ASF1-dependent pathways, or a compensatory reaction to the absence of ASF1. ASF1
633 is known to be involved in the recycling of histones during DNA replication (7). H3K27me3 is an
634 inheritable histone modification that can persist during replication and the *de novo* integration of
635 histones by ASF1 and CAF1 in parental cells was shown to heavily dilute the inheritance of this mark in
636 nascent chromatin in *A. thaliana* (68). Therefore, a reduction in *de novo* nucleosome assembly through
637 the deletion of a major histone chaperone like ASF1 could reduce general recycling of histones and
638 cause the already established H3K27me3 to persist and accumulate. Especially genomic regions that
639 do not carry H3K27me3 all the time under wild type conditions would show a visible increase under
640 such circumstances, matching our observations of significantly more uniquely marked positions in the
641 deletion mutant. Our observations for non-histone binding ASF1 variants and their deletion mutant-
642 like increase in H3K27me3 suggest a link between the histone interaction ability of ASF1 and the level
643 of H3K27me3 and support the idea that an ASF1, even if present as a protein but unable to interact
644 with histones and therefore probably unable to contribute to nucleosome recycling, may not be able
645 to prevent the persistence of H3K37me3. The blocking of nucleosome recycling and the resulting more
646 permanent marking of histones with H3K27me3 might be an explanation for the severe developmental
647 phenotype of *S. macrospora* Δasf1. Genome wide redistribution of H3K27me3 has been linked to
648 defects in sexual development in *N. crassa*, a close relative of *S. macrospora* (69), so the persistence
649 of this mark in regions where it would exist only temporarily in the wild type might cause similar
650 effects. However, the changes in H3K27me3 distribution could also be a reaction to the reduced DNA
651 methylation observed in Δasf1 (18). In addition to a global reduction of DNA methylation, the deletion

652 of the *S. macrospora asf1* leads to an increase in transcription of many usually weakly expressed genes
653 (18). DNA methylation and H3K27me3 are mostly considered to be marks of transcriptionally silenced
654 regions, but are often regarded as antagonistic to each other (70). Thus, the observed global increase
655 in H3K27me3 in a deletion mutant that also shows a decrease in DNA methylation could be the result
656 of a compensation mechanism for the loss of a transcriptional silencing mechanism. The rising
657 transcription levels resulting from the DNA methylation loss might be kept at least in an acceptable
658 range by using other transcriptional silencers, such as H3K27me3 to keep the deletion mutant alive.
659 This effect might therefore be one of the reasons why *S. macrospora* survives full *asf1* deletion and
660 other multicellular organisms do not.
661 Histone acetylations on the other hand are known as euchromatin markers, their negative charge can
662 lower the overall positive charge of histones and weaken their binding to the DNA. This can facilitate
663 a more relaxed and open chromatin state that can be accessed by RNA polymerases (71). The higher
664 transcription rates of usually weakly expressed genes after the deletion of *asf1* in *S. macrospora* might
665 suggest that euchromatin marks could be in higher abundance in such a strain. For H3K56ac, our
666 Western blot and ChIP-Seq results showed that at least for this mark, the opposite is the case and the
667 mutant exhibits less H3K56 acetylation on a global scale. As with the heterochromatin mark
668 H3K27me3, we were not able to detect specific patterns of acetylation loss, the overall abundance of
669 the mark appeared to be reduced. Strikingly, we still detected H3K56ac during western blot screenings,
670 as well as ChIP-Seq experiments, while it has been reported that the presence of ASF1 is required to
671 generate this mark in *S. cerevisiae* (72). Interestingly, our screens showed that the establishment of
672 H3K56ac seems to be related to the ability of ASF1 to interact with histones. Histone-binding defective
673 variants showed the same reduction in this mark as Δasf1 strains. Since this mark is generated by the
674 histone acetyltransferase RTT109, which is activated by ASF1 in *S. cerevisiae* (64), it can be speculated
675 that the lower abundance of H3K56ac results from a lack of ASF1-RTT109 interaction. It is speculated
676 that this interaction takes place in the form of a multi-protein complex consisting of ASF1, RTT109 and
677 the histones H3 and H4 together with additional factors (9). This may explain why, even in the presence
678 of ASF1, disruption of histone binding leads to loss of H3K56ac. Additionally, the presence of H3K56ac
679 in *S. macrospora* Δasf1, even though ASF1 was expected to be required for the generation of this mark,
680 hints at either an unknown second activation pathway for RTT109, or an undiscovered way to establish
681 H3K56ac in multicellular ascomycetes. Taken together with the detected increased levels of the
682 heterochromatin mark H3K27me3, lower euchromatic H3K56ac levels would suggest an all-around
683 lower general transcriptional activity of *S. macrospora asf1* deletion mutants. Since the opposite has
684 been documented (18), it can be hypothesized that the contribution of ASF1 to regulating the
685 transcriptome is either not mainly mediated by histone modifications, or is even more complex than
686 previously assumed.

687

688 **Hi-C analysis reveals a 600 kb duplication in *S. macrospora* Δasf1 which might be linked to its viability**

689 Methods such as Hi-C allow the analysis of the three-dimensional organization of the chromatin and
690 its effects on the transcriptome and gene regulation. The relationship between chromatin structure
691 and gene regulation seems to be quite complex and possibly both processes can regulate each other
692 (73). In this study, we created DNA-DNA interaction maps of the young, mostly vegetative state of *S.*
693 *macrospora* and compared it to older mycelium, which has progressed in the cycle of sexual
694 development and an *asf1* deletion mutant with the aim of identifying differences in the chromatin
695 state of those samples. The major challenge was the application of a method that has been fine tuned
696 for single cell assays and fungal protoplasts to older, more mature fungal mycelium. The resulting map
697 of the young wild type showed some areas of the chromatin that suggested higher condensation than
698 other areas, but in general the resolution was not high enough to confidently identify specific
699 interaction compartments. An even lower resolution was visible for the Hi-C map of the older, sexual
700 sample. *S. macrospora* mycelium grows thicker as it ages and sexual structures become reinforced by
701 melanization, which might further complicate the preparation of appropriate Hi-C samples.
702 Crosslinking might be less effective for such samples and the extraction of intact Hi-C pairs might be
703 impaired. The lower DNA-DNA interaction could also be a sign of multiple different chromatin states.
704 Entering sexual development, *S. macrospora* begins generating more specialized cell types, at least 13
705 different cell types have been identified during fruiting body formation of this fungus (4). Different
706 functions of cells require different transcriptomic processes, which can depend on specific changes of
707 the three-dimensional chromatin state. Higher differentiation of cells in a sample and therefore more
708 divergent chromatin states would reduce the signal-to-noise ratio and would lead to lower detection
709 rates of DNA-DNA interactions. Significant changes in the transcriptome during development are well
710 documented in *S. macrospora* (3). Other studies have demonstrated a strong connection between
711 detectable changes of chromatin architecture and gene expression (74), so it can be assumed that the
712 transcriptional changes of *S. macrospora* during sexual development might be accompanied by
713 significant changes of DNA-DNA interaction frequency. A lower resolution of regularly detectable
714 interactions in the older wild type that is generating multiple cell types supports these assumptions
715 and might be another sign of chromatin state changes that accompany multicellular development.

716 The Hi-C analysis of the Δasf1 mutant revealed a large duplicated region on chromosome 2. We
717 hypothesized that the presence of this duplication might not be just a coincidence, but could be linked
718 to the surprising viability of the Δasf1 mutant in *S. macrospora*. Genetic crosses confirmed co-
719 segregation of the Δasf1 allele on chromosome 6 with the duplication on chromosome 2, whereas the
720 wild type *asf1* allele and the duplication were able to recombine freely. These findings support the
721 hypothesis that the viability of the Δasf1 mutant is coupled to the presence of the duplication. Which

722 specific role this region on chromosome 2 plays in the network of ASF1 is still unclear. So far, no
723 documented interaction partners or parts of the ASF1 network seem to be encoded in this region. The
724 duplication itself seems to be irrelevant for strains expressing *asf1*, even if the ASF1 variant is non-
725 functional with respect to histone binding and sexual development. Strains expressing *asf1* with V94R
726 substitution or truncations after amino acids 185 or 152 were viable but sterile with or without the
727 duplication, and wild type and D37A strains were fertile and did not show additional phenotypes when
728 the duplication was present. One hypothesis might be that the duplication somehow contributes to
729 DNA damage repair or protection, since MMS resistance is the only phenotype that V94R, 185T and
730 152T confer compared to the *asf1* deletion mutant.
731 Summarizing our work, we discovered that the ability of ASF1 to interact with histones is essential for
732 sexual development of *S. macrospora*, a function that also depends on the presence of large part of
733 the less conserved C-terminus of ASF1. Histone binding however, proved not to be necessary to allow
734 ASF1 to contribute to the genotoxic stress response. ChIP-seq experiments showed that ASF1 is
735 involved in the establishment of H3K56ac and the repression of H3K27me3. Furthermore, we
736 discovered a 600 kb duplication in the deletion mutant that appears to be linked to the viability of *S.*
737 *macrospora* Δasf1. Future work might be able to shed light on how ASF1 regulates gene expression by
738 histone modification and which genes of the duplicated area are necessary to stabilize *asf1* deletion
739 mutants.
740
741
742 **Acknowledgements**
743 The authors would like to thank Silke Nimtz, Susanne Schlewinski and Tanja Rollnik for excellent
744 technical assistance and Christopher Grefen for support at the Department of Molecular and Cellular
745 Botany. The authors acknowledge the NGS team of the Omics CF NGS Unit (in development) and
746 CeBiTec. This work was funded by the German Research Foundation (DFG, grant NO407/7-2 to MN).
747 We acknowledge support by the Open Access Publication Funds of the Ruhr-Universität Bochum
748
749
750 **References**
751 1. Niklas KJ, Newman SA. 2020. The many roads to and from multicellularity. Journal of
752 Experimental Botany 71:3247-3253.
753 2. Nagy LG, Kovács GM, Krizsán K. 2018. Complex multicellularity in fungi: evolutionary
754 convergence, single origin, or both? Biol Rev 93:1778-1794.
755 3. Teichert I, Pöggeler S, Nowrousian M. 2020. *Sordaria macrospora*: 25 years as a model
756 organism for studying the molecular mechanisms of fruiting body development. Appl
757 Microbiol Biotechnol 104:3691-3704.
758 4. Lord KM, Read ND. 2011. Perithecium morphogenesis in *Sordaria macrospora*. Fungal Genet
759 Biol 48:388-99.

760 5. Nowrousian M. 2018. Genomics and transcriptomics to study fruiting body development: An
761 update. Fungal Biology Reviews 32:231-235.
762 6. Gesing S, Schindler D, Fränzel B, Wolters D, Nowrousian M. 2012. The histone chaperone ASF1
763 is essential for sexual development in the filamentous fungus *Sordaria macrospora*. Mol
764 Microbiol 84:748-65.
765 7. English CM, Adkins MW, Carson JJ, Churchill ME, Tyler JK. 2006. Structural basis for the histone
766 chaperone activity of ASF1. Cell 127:495-508.
767 8. Yamane K, Mizuguchi T, Cui B, Zofall M, Noma K, Grewal SI. 2011. ASF1/HIRA facilitate global
768 histone deacetylation and associate with HP1 to promote nucleosome occupancy at
769 heterochromatic loci. Mol Cell 41:56-66.
770 9. Lercher L, Danilenko N, Kirkpatrick J, Carlomagno T. 2018. Structural characterization of the
771 ASF1-RTT109 interaction and its role in histone acetylation. Nucleic Acids Res 46:2279-2289.
772 10. Clément C, Orsi GA, Gatto A, Boyarchuk E, Forest A, Hajj B, Miné-Hattab J, Garnier M, Gurard-
773 Levin ZA, Quivy J-P, Almouzni G. 2018. High-resolution visualization of H3 variants during
774 replication reveals their controlled recycling. Nature Communications 9:3181.
775 11. Prado F, Cortés-Ledesma F, Aguilera A. 2004. The absence of the yeast chromatin assembly
776 factor ASF1 increases genomic instability and sister chromatid exchange. EMBO Rep 5:497-
777 502.
778 12. Groth A, Ray-Gallet D, Quivy J-P, Lukas J, Bartek J, Almouzni G. 2005. Human ASF1 Regulates
779 the Flow of S Phase Histones during Replicational Stress. Molecular Cell 17:301-311.
780 13. Tagami H, Ray-Gallet D, Almouzni G, Nakatani Y. 2004. Histone H3.1 and H3.3 complexes
781 mediate nucleosome assembly pathways dependent or independent of DNA synthesis. Cell
782 116:51-61.
783 14. Le S, Davis C, Konopka JB, Sternglanz R. 1997. Two new S-phase-specific genes from
784 *Saccharomyces cerevisiae*. Yeast 13:1029-1042.
785 15. Singer MS, Kahana A, Wolf AJ, Meisinger LL, Peterson SE, Goggin C, Mahowald M, Gottschling
786 DE. 1998. Identification of high-copy disruptors of telomeric silencing in *Saccharomyces*
787 *cerevisiae*. Genetics 150:613-32.
788 16. Tyler JK, Adams CR, Chen SR, Kobayashi R, Kamakaka RT, Kadonaga JT. 1999. The RCAF complex
789 mediates chromatin assembly during DNA replication and repair. Nature 402:555-60.
790 17. Zhu Y, Weng M, Yang Y, Zhang C, Li Z, Shen WH, Dong A. 2011. *Arabidopsis* homologues of the
791 histone chaperone ASF1 are crucial for chromatin replication and cell proliferation in plant
792 development. Plant J 66:443-55.
793 18. Schumacher DI, Lütkenhaus R, Altegoer F, Teichert I, Kück U, Nowrousian M. 2018. The
794 transcription factor PRO44 and the histone chaperone ASF1 regulate distinct aspects of
795 multicellular development in the filamentous fungus *Sordaria macrospora*. BMC Genetics
796 19:112.
797 19. Mousson F, Lautrette A, Thuret JY, Agez M, Courbeyrette R, Amigues B, Becker E, Neumann
798 JM, Guerois R, Mann C, Ochsenbein F. 2005. Structural basis for the interaction of ASF1 with
799 histone H3 and its functional implications. Proc Natl Acad Sci U S A 102:5975-80.
800 20. Esser K. Cryptogams : cyanobacteria, algae, fungi, lichens : textbook and practical guide, p. *In*
801 (ed),
802 21. Walz M, Kück U. 1995. Transformation of *Sordaria macrospora* to hygromycin B resistance:
803 characterization of transformants by electrophoretic karyotyping and tetrad analysis. Curr
804 Genet 29:88-95.
805 22. Kück U, Pöggeler S, Nowrousian M, Nolting N, Teichert I. 2009. *Sordaria macrospora*, a Model
806 System for Fungal Development, p 17-39 doi:10.1007/978-3-642-00286-1_2.
807 23. Oldenburg KR, Vo KT, Michaelis S, Paddon C. 1997. Recombination-mediated PCR-directed
808 plasmid construction *in vivo* in yeast. Nucleic Acids Res 25:451-2.
809 24. Terfrüchte M, Joehnk B, Fajardo-Somera R, Braus GH, Riquelme M, Schipper K, Feldbrügge M.
810 2014. Establishing a versatile Golden Gate cloning system for genetic engineering in fungi.
811 Fungal Genet Biol 62:1-10.

25. Nowrousian M, Masloff S, Pöggeler S, Kück U. 1999. Cell differentiation during sexual development of the fungus *Sordaria macrospora* requires ATP citrate lyase activity. Mol Cell Biol 19:450-460.
26. Bayram O, Krappmann S, Ni M, Bok JW, Helmstaedt K, Valerius O, Braus-Stromeyer S, Kwon NJ, Keller NP, Yu JH, Braus GH. 2008. VelB/VeA/LaeA complex coordinates light signal with fungal development and secondary metabolism. Science 320:1504-6.
27. Laemmli UK. 1970. Cleavage of structural proteins during the assembly of the head of bacteriophage T4. Nature 227:680-5.
28. Colot HV, Park G, Turner GE, Ringelberg C, Crew CM, Litvinkova L, Weiss RL, Borkovich KA, Dunlap JC. 2006. A high-throughput gene knockout procedure for Neurospora reveals functions for multiple transcription factors. Proc Nat Acad Sci USA 103:10352-10357.
29. Engh I, Würtz C, Witzel-Schlömp K, Zhang Hai Y, Hoff B, Nowrousian M, Rottensteiner H, Kück U. 2007. The WW Domain Protein PRO40 Is Required for Fungal Fertility and Associates with Woronin Bodies. Eukaryotic Cell 6:831-843.
30. Traeger S, Altegoer F, Freitag M, Gabaldon T, Kempken F, Kumar A, Marcet-Houben M, Pöggeler S, Stajich JE, Nowrousian M. 2013. The genome and development-dependent transcriptomes of *Pyronema confluens*: a window into fungal evolution. PLoS Genet 9:e1003820.
31. Vaser R, Sović I, Nagarajan N, Šikić M. 2017. Fast and accurate de novo genome assembly from long uncorrected reads. Genome Res 27:737-746.
32. Walker BJ, Abeel T, Shea T, Priest M, Abouelliel A, Sakthikumar S, Cuomo CA, Zeng Q, Wortman J, Young SK, Earl AM. 2014. Pilon: an integrated tool for comprehensive microbial variant detection and genome assembly improvement. PLOS ONE 9:e112963.
33. Blank-Landeshammer B, Teichert I, Märker R, Nowrousian M, Kück U, Sickmann A. 2019. Combination of proteogenomics with peptide *de novo* sequencing identifies new genes and hidden posttranscriptional modifications. mBio 10:e02367-19.
34. Altschul SF, Madden TL, Schaffer AA, Zhang J, Zhang Z, Miller W, Lipman DJ. 1997. Gapped BLAST and PSI-BLAST: a new generation of protein database search programs. Nucleic Acids Res 25:3389-3402.
35. Nowrousian M, Stajich JE, Chu M, Engh I, Espagne E, Halliday K, Kamerewerd J, Kempken F, Knab B, Kuo HC, Osiewacz HD, Pöggeler S, Read ND, Seiler S, Smith KM, Zickler D, Kück U, Freitag M. 2010. *De novo* assembly of a 40 Mb eukaryotic genome from short sequence reads: *Sordaria macrospora*, a model organism for fungal morphogenesis. PLoS Genet 6:e1000891.
36. Sović I, Šikić M, Wilm A, Fenlon SN, Chen S, Nagarajan N. 2016. Fast and sensitive mapping of nanopore sequencing reads with GraphMap. Nat Commun 7:11307.
37. Basenko EY, Pulman JA, Shanmugasundram A, Harb OS, Crouch K, Starns D, Warrenfeltz S, Aurrecoechea C, Stoeckert CJJ, Kissinger J, Roos DS, Hertz-Fowler C. 2018. FungiDB: An integrated bioinformatic resource for fungi and oomycetes. J Fungi 4:39.
38. Galagan JE, Calvo SE, Borkovich KA, Selker EU, Read ND, Jaffe D, FitzHugh W, Ma LJ, Smirnov S, Purcell S, Rehman B, Elkins T, Engels R, Wang S, Nielsen CB, Butler J, Endrizzi M, Qui D, Ianakiev P, Bell-Pedersen D, Nelson MA, Werner-Washburne M, Selitrennikoff CP, Kinsey JA, Braun EL, Zelter A, Schulte U, Kothe GO, Jedd G, Mewes W, Staben C, Marcotte E, Greenberg D, Roy A, Foley K, Naylor J, Stange-Thomann N, Barrett R, Gnerre S, Kamal M, Kamvysselis M, Mauceli E, Bielke C, Rudd S, Frishman D, Krystofova S, Rasmussen C, Metzenberg RL, Perkins DD, Kroken S, et al. 2003. The genome sequence of the filamentous fungus *Neurospora crassa*. Nature 422:859-868.
39. Kurtz S, Phillippy A, Delcher AL, Smoot M, Shumway M, Antonescu C, Salzberg SL. 2004. Versatile and open software for comparing large genomes. Genome Biol 5:R12.
40. Cantarel BL, Korf I, Robb SMC, Parra G, Ross E, Moore B, Holt C, Sánchez Alvarado A, Yandell M. 2008. MAKER: An easy-to-use annotation pipeline designed for emerging model organism genomes. Genome Res 18:188-196.

863 41. Lowe TM, Eddy SR. 1997. tRNAscan-SE: a program for improved detection of transfer RNA
864 genes in genomic sequence. Nucl Acids Res 25:955-964.
865 42. Carver T, Harris SR, Berriman M, Parkhill J, McQuillan JA. 2012. Artemis: an integrated platform
866 for visualization and analysis of high-throughput sequence-based experimental data. Bioinf
867 28:464-469.
868 43. Teichert I, Wolff G, Kück U, Nowrousian M. 2012. Combining laser microdissection and RNA-
869 seq to chart the transcriptional landscape of fungal development. BMC Genomics 13:511.
870 44. Kim D, Paggi JM, Park C, Bennett C, Salzberg SL. 2019. Graph-based genome alignment and
871 genotyping with HISAT2 and HISAT-genotype. Nat Biotech 37:907-915.
872 45. Bradford MM. 1976. A rapid and sensitive method for the quantitation of microgram quantities
873 of protein utilizing the principle of protein-dye binding. Analytical Biochemistry 72:248-254.
874 46. Huang X, Pan Q, Lin Y, Gu T, Li Y. 2020. A native chromatin immunoprecipitation (ChIP) protocol
875 for studying histone modifications in strawberry fruits. Plant Methods 16:10.
876 47. Chen S, Zhou Y, Chen Y, Gu J. 2018. fastp: an ultra-fast all-in-one FASTQ preprocessor.
877 Bioinformatics 34:i884-i890.
878 48. Li H, Durbin R. 2010. Fast and accurate long-read alignment with Burrows–Wheeler transform.
879 Bioinformatics 26:589-595.
880 49. Schulten A, Pietzenuk B, Quintana J, Scholle M, Feil R, Krause M, Romera-Branchat M, Wahl V,
881 Severing E, Coupland G, Krämer U. 2022. Energy status-promoted growth and development of
882 Arabidopsis require copper deficiency response transcriptional regulator SPL7. Plant Cell
883 34:3873-3898.
884 50. Zhang Y, Liu T, Meyer CA, Eeckhoute J, Johnson DS, Bernstein BE, Nusbaum C, Myers RM,
885 Brown M, Li W, Liu XS. 2008. Model-based Analysis of ChIP-Seq (MACS). Genome Biology
886 9:R137.
887 51. Quinlan AR, Hall IM. 2010. BEDTools: a flexible suite of utilities for comparing genomic
888 features. Bioinformatics 26:841-842.
889 52. Heinz S, Benner C, Spann N, Bertolino E, Lin YC, Laslo P, Cheng JX, Murre C, Singh H, Glass CK.
890 2010. Simple Combinations of Lineage-Determining Transcription Factors Prime cis-Regulatory
891 Elements Required for Macrophage and B Cell Identities. Molecular Cell 38:576-589.
892 53. Open2C, Nezar A, Geoffrey F, Ilya MF, Aleksandra AG, Anton G, Maxim I, Sergey VV. 2023.
893 Pairtools: from sequencing data to chromosome contacts. bioRxiv
894 doi:10.1101/2023.02.13.528389:2023.02.13.528389.
895 54. Durand NC, Shamim MS, Machol I, Rao SS, Huntley MH, Lander ES, Aiden EL. 2016. Juicer
896 Provides a One-Click System for Analyzing Loop-Resolution Hi-C Experiments. Cell Syst 3:95-8.
897 55. Nowrousian M, Teichert I, Masloff S, Kück U. 2012. Whole-genome sequencing of *Sordaria*
898 *macrospora* mutants identifies developmental genes. G3 (Bethesda) 2:261-270.
899 56. Nowrousian M, Würtz C, Pöggeler S, Kück U. 2004. Comparative sequence analysis of *Sordaria*
900 *macrospora* and *Neurospora crassa* as a means to improve genome annotation. Fungal Genet
901 Biol 41:285-292.
902 57. Malay AD, Umehara T, Matsubara-Malay K, Padmanabhan B, Yokoyama S. 2008. Crystal
903 structures of fission yeast histone chaperone Asf1 complexed with the Hip1 B-domain or the
904 Cac2 C terminus. Journal of Biological Chemistry 283:14022-14031.
905 58. Daganzo SM, Erzberger JP, Lam WM, Skordalakes E, Zhang R, Franco AA, Brill SJ, Adams PD,
906 Berger JM, Kaufman PD. 2003. Structure and function of the conserved core of histone
907 deposition protein ASF1. Curr Biol 13:2148-58.
908 59. Dennehey BK, Noone S, Liu WH, Smith L, Churchill ME, Tyler JK. 2013. The C terminus of the
909 histone chaperone ASF1 cross-links to histone H3 in yeast and promotes interaction with
910 histones H3 and H4. Mol Cell Biol 33:605-21.
911 60. Tamburini BA, Carson JJ, Linger JG, Tyler JK. 2006. Dominant mutants of the *Saccharomyces*
912 *cerevisiae* ASF1 histone chaperone bypass the need for CAF-1 in transcriptional silencing by
913 altering histone and Sir protein recruitment. Genetics 173:599-610.

914 61. Landt SG, Marinov GK, Kundaje A, Kheradpour P, Pauli F, Batzoglou S, Bernstein BE, Bickel P,
915 Brown JB, Cayting P, Chen Y, DeSalvo G, Epstein C, Fisher-Aylor KI, Euskirchen G, Gerstein M,
916 Gertz J, Hartemink AJ, Hoffman MM, Iyer VR, Jung YL, Karmakar S, Kellis M, Kharchenko PV, Li
917 Q, Liu T, Liu XS, Ma L, Milosavljevic A, Myers RM, Park PJ, Pazin MJ, Perry MD, Raha D, Reddy
918 TE, Rozowsky J, Shoresh N, Sidow A, Slattery M, Stamatoyannopoulos JA, Tolstorukov MY,
919 White KP, Xi S, Farnham PJ, Lieb JD, Wold BJ, Snyder M. 2012. ChIP-seq guidelines and practices
920 of the ENCODE and modENCODE consortia. Genome Res 22:1813-31.
921 62. Tang M, Chen Z, Wang C, Feng X, Lee N, Huang M, Zhang H, Li S, Xiong Y, Chen J. 2022. Histone
922 chaperone ASF1 acts with RIF1 to promote DNA end joining in BRCA1-deficient cells. Journal
923 of Biological Chemistry 298:101979.
924 63. Mao P, Wyrick JJ. 2016. Emerging roles for histone modifications in DNA excision repair. FEMS
925 Yeast Research 16:fow090.
926 64. Tsubota T, Berndsen CE, Erkmann JA, Smith CL, Yang L, Freitas MA, Denu JM, Kaufman PD.
927 2007. Histone H3-K56 acetylation is catalyzed by histone chaperone-dependent complexes.
928 Mol Cell 25:703-12.
929 65. Tsabar M, Waterman DP, Aguilar F, Katsnelson L, Eapen VV, Memisoglu G, Haber JE. 2016. ASF1
930 facilitates dephosphorylation of RAD53 after DNA double-strand break repair. Genes Dev
931 30:1211-24.
932 66. Bannister AJ, Kouzarides T. 2011. Regulation of chromatin by histone modifications. Cell Res
933 21:381-95.
934 67. Boros J, Arnoult N, Stroobant V, Collet JF, Decottignies A. 2014. Polycomb repressive complex
935 2 and H3K27me3 cooperate with H3K9 methylation to maintain heterochromatin protein 1α
936 at chromatin. Mol Cell Biol 34:3662-74.
937 68. Hugues A, Jacobs CS, Roudier F. 2020. Mitotic Inheritance of PRC2-Mediated Silencing:
938 Mechanistic Insights and Developmental Perspectives. Frontiers in Plant Science 11.
939 69. Basenko EY, Sasaki T, Ji L, Prybol CJ, Burckhardt RM, Schmitz RJ, Lewis ZA. 2015. Genome-wide
940 redistribution of H3K27me3 is linked to genotoxic stress and defective growth. Proc Natl Acad
941 Sci U S A 112:E6339-48.
942 70. Hagarman JA, Motley MP, Kristjansdottir K, Soloway PD. 2013. Coordinate regulation of DNA
943 methylation and H3K27me3 in mouse embryonic stem cells. PLoS One 8:e53880.
944 71. Lee CY, Grant PA. 2019. Chapter 1-1 - Role of Histone Acetylation and Acetyltransferases in
945 Gene Regulation, p 3-30. *In* McCullough SD, Dolinoy DC (ed), Toxicoepigenetics
946 doi:https://doi.org/10.1016/B978-0-12-812433-8.00001-0. Academic Press.
947 72. Adkins MW, Carson JJ, English CM, Ramey CJ, Tyler JK. 2007. The Histone Chaperone Anti-
948 silencing Function 1 Stimulates the Acetylation of Newly Synthesized Histone H3 in S-phase*.
949 Journal of Biological Chemistry 282:1334-1340.
950 73. Banigan EJ, Tang W, van den Berg AA, Stocsits RR, Wutz G, Brandão HB, Busslinger GA, Peters
951 J-M, Mirny LA. 2023. Transcription shapes 3D chromatin organization by interacting with loop
952 extrusion. Proceedings of the National Academy of Sciences 120:e2210480120.
953 74. Almassalha LM, Tiwari A, Ruhoff PT, Stypula-Cyrus Y, Cherkezyan L, Matsuda H, Dela Cruz MA,
954 Chandler JE, White C, Maneval C, Subramanian H, Szleifer I, Roy HK, Backman V. 2017. The
955 Global Relationship between Chromatin Physical Topology, Fractal Structure, and Gene
956 Expression. Sci Rep 7:41061.

957

958

959 **Tables**

960

961 **Table 1.** Transformants in complementation experiments of ∆asf1 with ASF1 variants.

Encoded ASF1 variant	No. of primary transformants	Fertile transformants	Sterile transformants	Percentage of fertile transformants
Wild type	53	47	6	88.7
D37A	61	41	20	67.2
V94R	41	0	41	0
152T	19	0	19	0
185T	22	0	22	0
210T	18	15	3	83.3

962

963

964 **Table 2.** Presence of the duplication on chromosome 2 in wild type, *asf1* deletion strains and strains
965 expressing *asf1* variants. Strains were obtained from crosses of ∆asf1 with the spore color mutant fus,
966 which carries the wild type *asf1* gene. The full list of tested strains has been added as Supplemental
967 table 9.

Genotype	No. of tested strains	No. of strains with duplication	Percentage of strains with duplication
Wild type	69	21	30.4
Δasf1	42	42	100
Δasf1 + *asf1* D37A	7	2	28.6
Δasf1 + *asf1* V94R	15	5	30
Δasf1 + *asf1* 152T	5	2	40
Δasf1 + *asf1* 185T	9	2	22.2

968

969

Figures

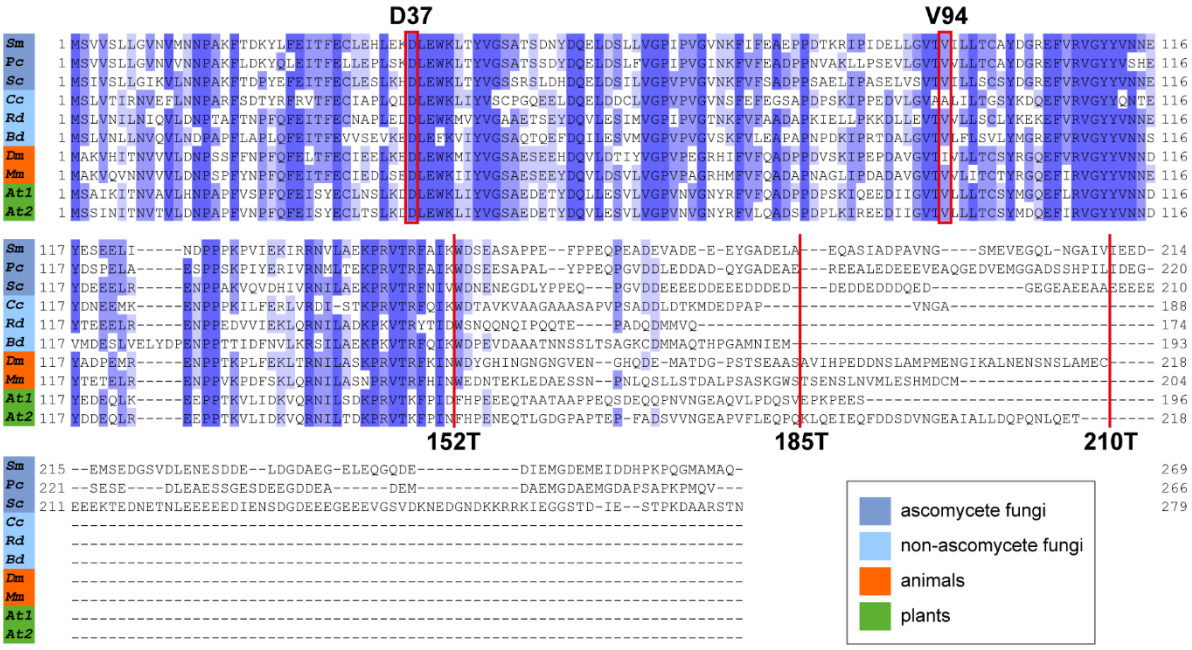

Figure 1. Alignment of ASF1 amino acid sequences from fungi, animals and plant. The first 152 amino acids are highly conserved. The C-terminal region is more divergent and parts of it exist only in ascomycete fungi. Positions D37 and V94 were substituted for functional analysis in this study. D37 is known as a HIRA interaction site in *Schizosaccharomyces pombe* (57), while V94 has been established as the H3-H4 interaction site (7, 19). Positions 152, 185 and 210 were targeted to create truncated ASF1 variants. Abbreviations and accession numbers: Ascomycetes: *Sm*, *Sordaria macrospora* (KAA8632619.1); *Pc*, *Pyronema confluens* (ADZ55332.1); *Sc*, *Saccharomyces cerevisiae* (NP_012420.1). Basidiomycetes: *Cc*, *Coprinopsis cinerea* (XP_001834011.1). Mucoromycetes: *Rd*, *Rhizopus delemar* (EIE83079.1). Chytridiomycetes: *Bd*, *Batrachochytrium dendrobatidis* (KAJ8331661.1). Animals: *Dm*, *Drosophila melanogaster* (NP_524163.1); *Mm*, *Mus musculus* (AAH27628.1). Plants: *At*, *Arabidopsis thaliana* (NP_176846.1 and NP_198627.1). The taxonomic groups are color coded according to the legend in the figure.

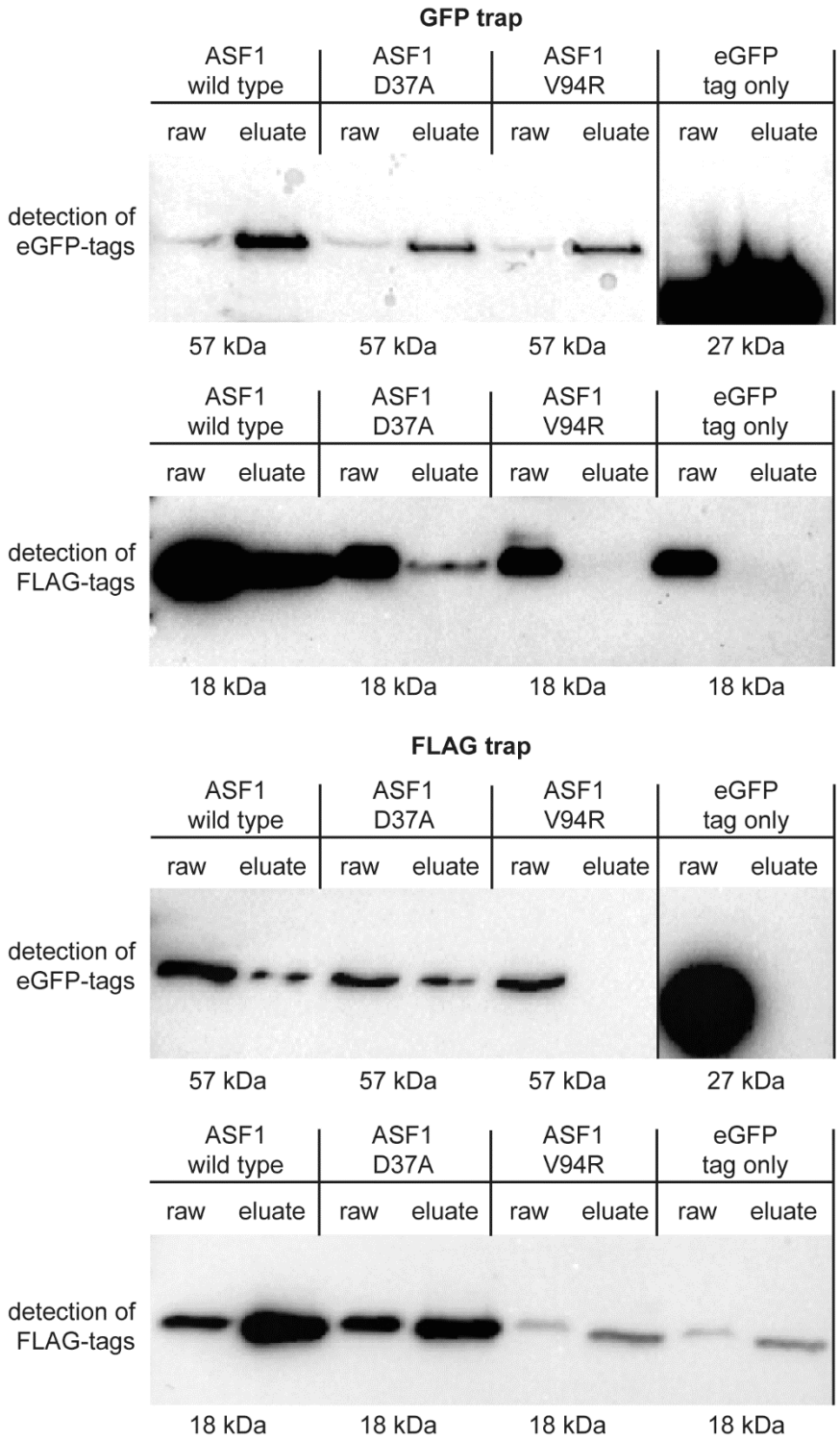

Figure 2. Co-immunoprecipitation results for ASF1 variants with amino acid substitutions and histone H3. GFP-tagged ASF1 wild type and variants D37A and V94R were used as potential interaction partners for Flag-tagged histone H3 in a GFP trap and a Flag trap. Results were checked by western blot analysis with antibodies against GFP and Flag tags. ASF1 wild type and the D37A variant showed signals for bait and prey proteins in the raw and eluate sample, indicating interaction, whereas the V94R variant showed the signal for the prey protein only in the raw sample. Strains expressing non-fused GFP with the corresponding Flag-tagged H3 were used as a negative control. Results for histone H4 are shown in Supplemental Figure 2. Uncropped blots are shown in Supplemental Figure 3A.

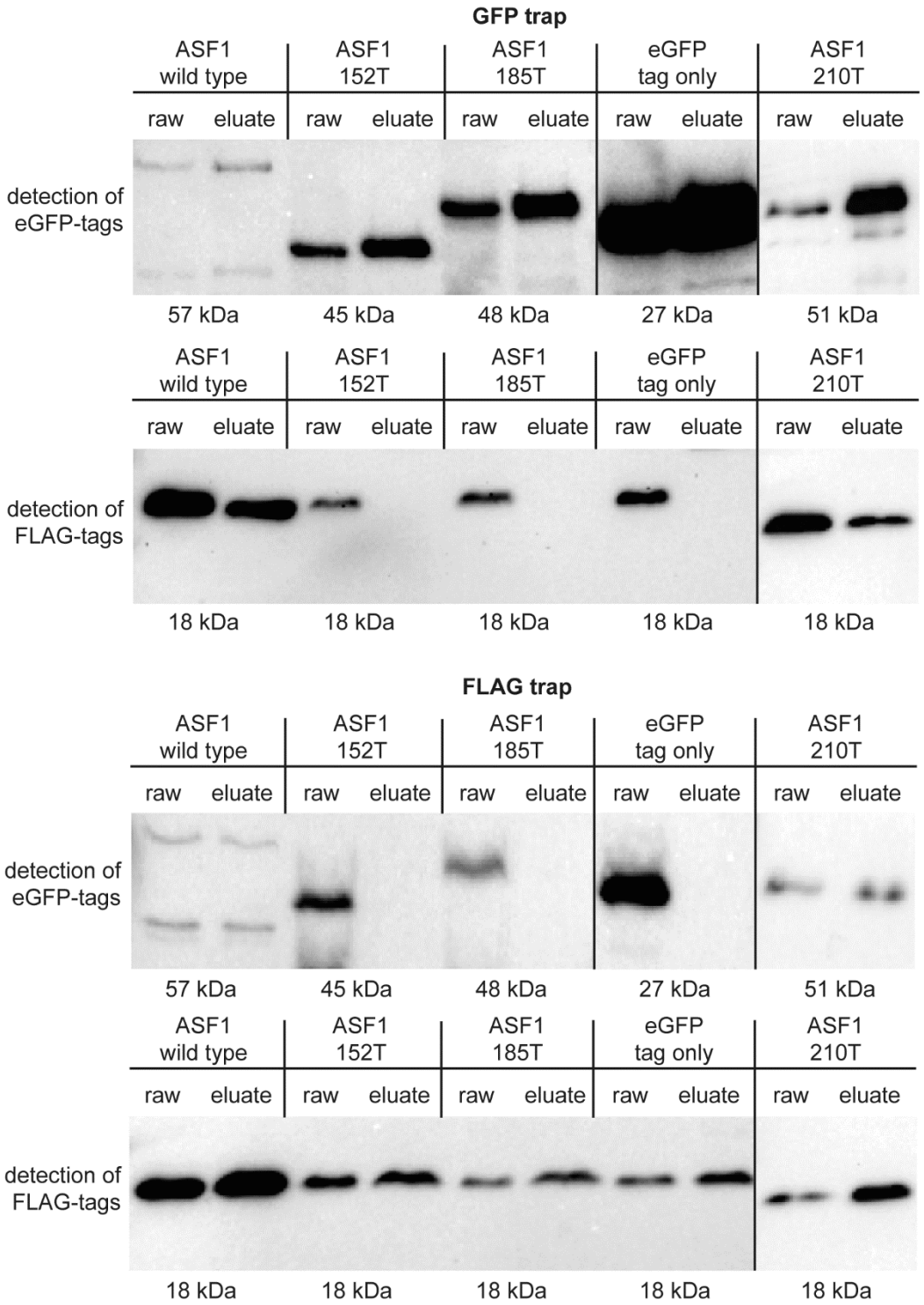

Figure 3. Co-immunoprecipitation results for truncated ASF1 variants and histone H3. GFP-tagged ASF1 wild type and variants 152T, 185T and 210T were used as potential interaction partners for Flag-tagged histone H3 in a GFP trap and a Flag trap. Results were checked by western blot analysis with antibodies against GFP and Flag tags. ASF1 wild type and the 210T variant showed signals for bait and prey proteins in the raw and eluate sample, indicating interaction, whereas the 152T and 185T variants showed the signal for the prey protein only in the raw sample. Strains expressing non-fused GFP with the corresponding Flag-tagged H3 were used as a negative control. Results for histone H4 are shown in Supplemental Figure 4. Uncropped blots are shown in Supplemental figure 5A.

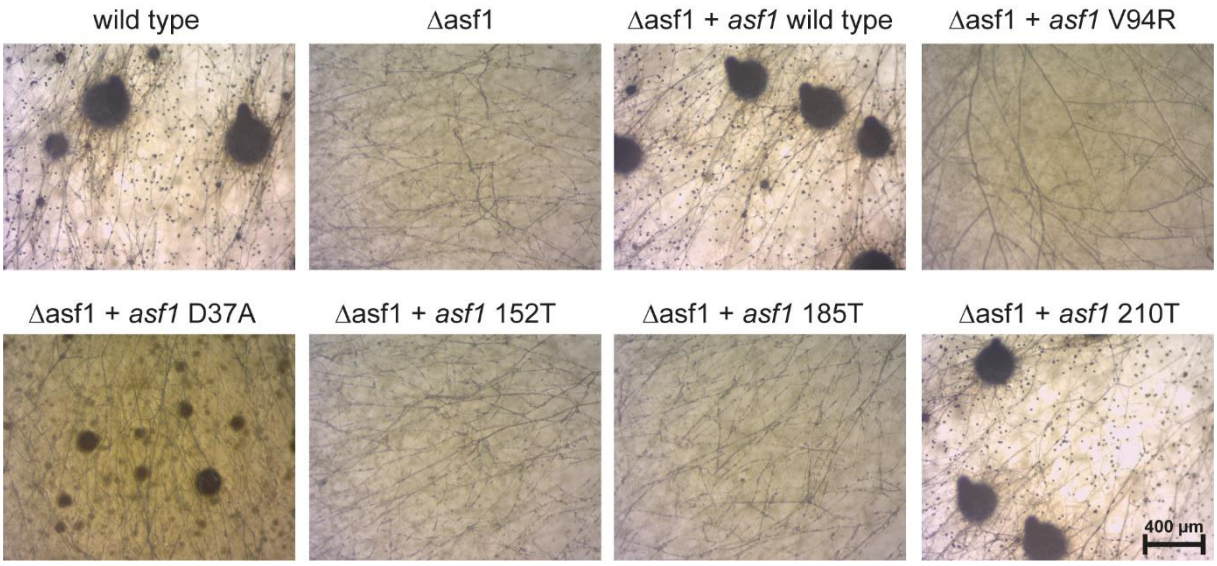

Figure 4. Phenotypes of strains from Δasf1 complementation experiments. The wild type generates mature perithecia in 7 days, while the development of the deletion mutant is blocked at the stage of early protoperithecia and mostly generates only vegetative mycelium. Reintroducing the *asf1* wild type gene into the deletion mutant fully complements the phenotype and lead to strains that are indistinguishable from the wild type. Transforming Δasf1 with the *asf1* V94R variant did not complement the mutant strain resulting in strains with the sterile phenotype of Δasf1. A D37A variant partially complements the mutant, such strains are fertile, but show distinct developmental aberrations like a tendency to generate mostly large protoperithecia and a brown coloration of the mycelium. Transformation with truncated *asf1* variants did not lead to complementation with variants 152T and 185T, but the longer 210T variant led to strains that show a wild type phenotype again.

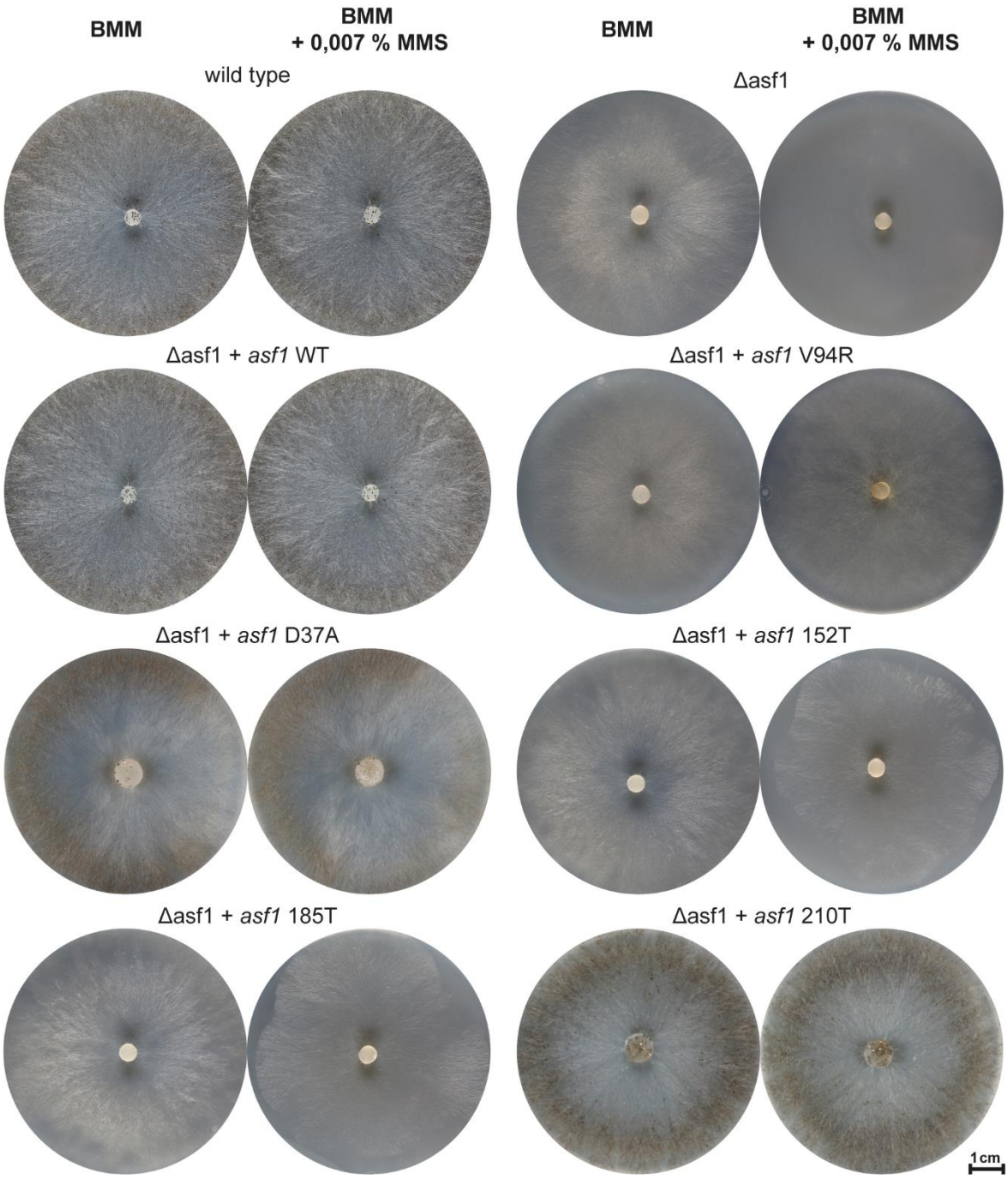

Figure 5. Genotoxic stress resistance of *S. macrospora* strains expressing ASF1 variants. At the given MMS concentration, the wild type was able to grow normally, while the *asf1* deletion mutant exhibited severe sensitivity (no growth). Reintroducing the wild type *asf1* into the mutant restored the resistance. All strains that expressed any kind of ASF1 variant showed at least partial resistance to genotoxic stress, even variants that were shown to be unable to interact with histones and do not complement the developmental defects of *S. macrospora* Δasf1.

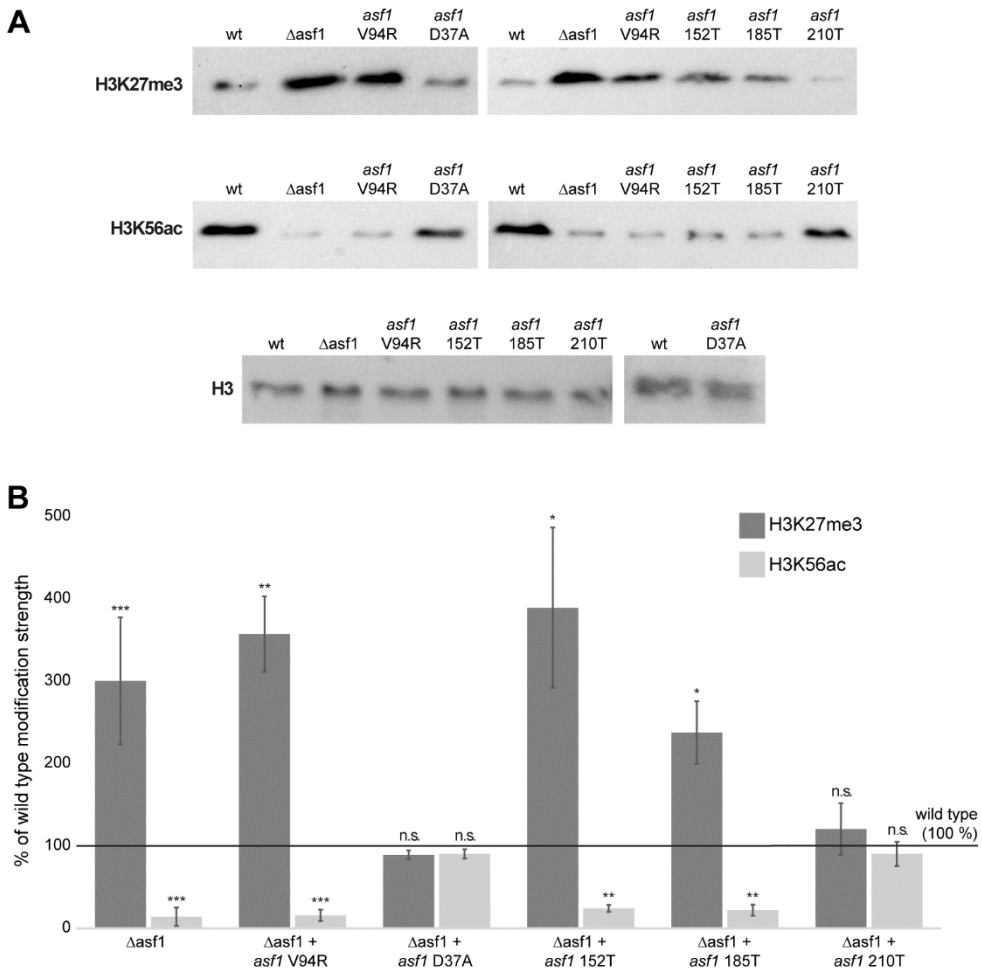

Figure 6. Semiquantitative screening for histone modifications affected by ASF1.

A. Western blots with antibodies against the indicated histone modifications were used to compare the band strength of equal amounts of protein from wild type, Δasf1 and strains expressing *asf1* variants. H3 levels were measured as an internal control. Uncropped blots are included in Supplemental Figure 10.

B. Band intensity in Western blots was measured densitometrically and the ratio of mutants to wild type was calculated. The deletion mutant as well as the non-histone binding variants showed a significant increase in H3K27me3 and a significant decrease in H3K56ac. N wild type and Δasf1 = 9; N *asf1* variants = 3. Student's t-test for significance: * = p-value < 0.05; ** = p-value < 0.01.

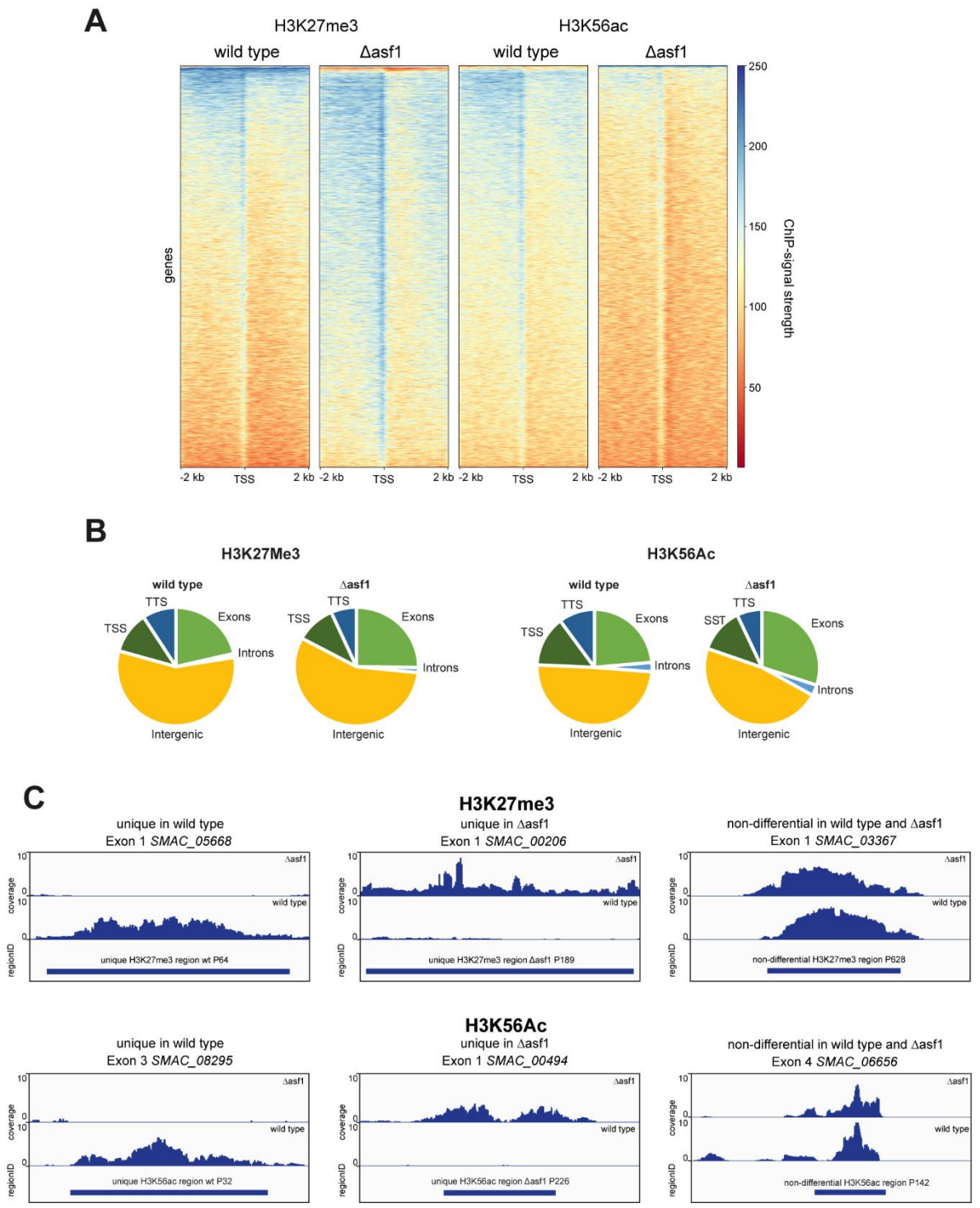

Figure 7. Analysis of histone modifications in the wild type, Δasf1 and *asf1* variants.

A. Heatmap showing ChIP signal strength at regions surrounding transcription start sites (TSS) in wild type and deletion mutant. *S. macrospora* Δasf1 shows an increase in H3K27me3 and a decrease in H3K56ac compared to the wild type.

B. Relative distribution of H3K27me3 and H3K56ac in annotated regions of *S. macrospora* in wild type and Δasf1. Although the general amount of both marks underwent significant changes in the deletion mutant, we did not observe a significant change in the relative positioning of H3K27Me3 or H3K56ac, although a slight shift into exonic regions appears likely.

1053 **C.** Representative exon regions exhibiting H3K27me3 and H3K56ac. The coverage in the wild type and
1054 deletion mutant is shown in the respective area for a unique region in the wild type and the deletion
1055 mutant, as well as for a non-differential exon region. Representative regions for introns, promoter
1056 regions, downstream regions, and intergenic regions are shown in Supplemental Figures 15 A-C.
1057

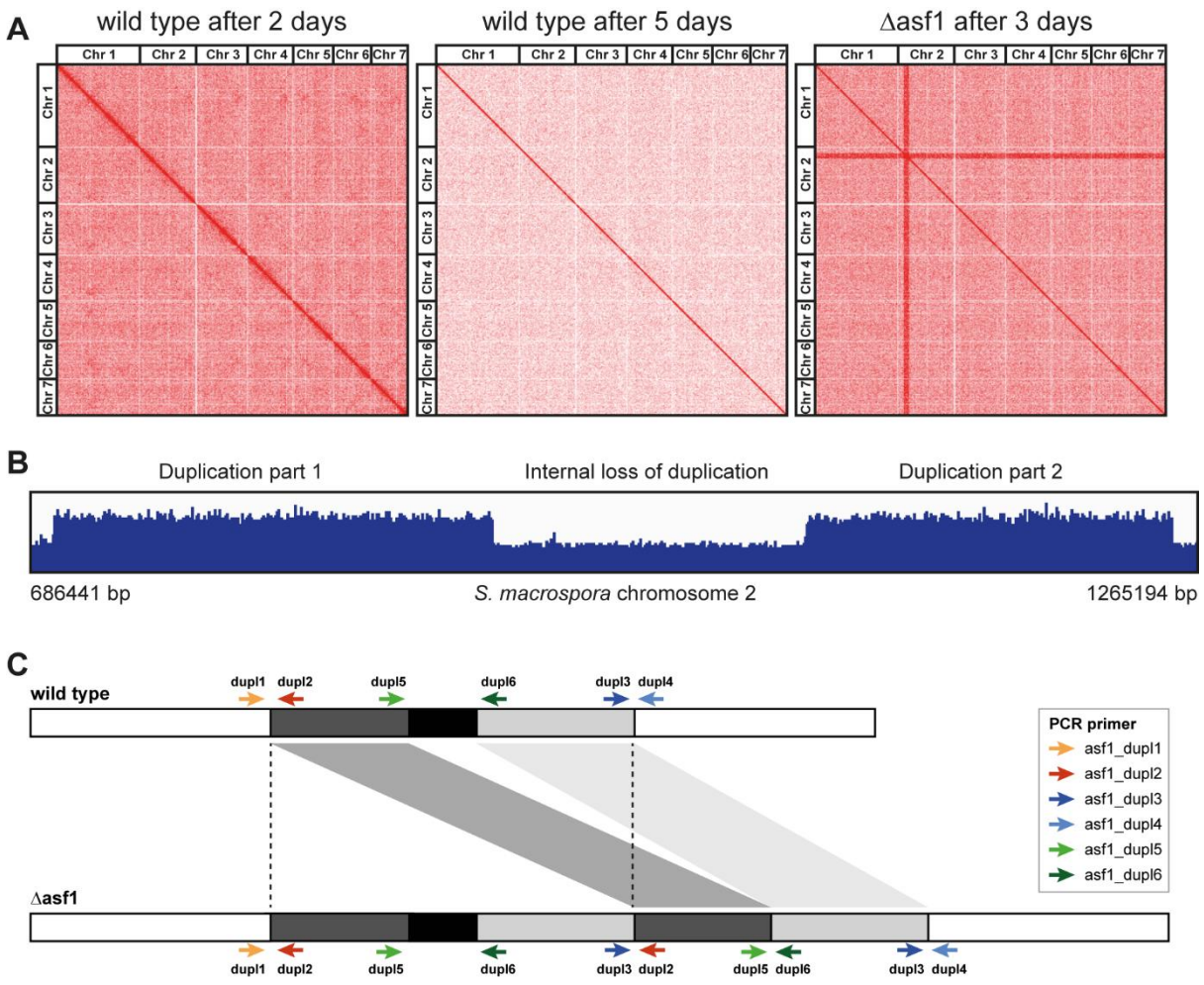

Figure 8. Detection of a 600kb duplication in *S. macrospora* Δasf1 by Hi-C and genome sequencing. **A.** Hi-C analysis of *S. macrospora* wild type and Δasf1. DNA-DNA interactions recorded in the samples at the given time were plotted against both interacting positions in the genome. Each red dot represents an interaction event. The characteristic red diagonal indicates highly increased interaction frequencies of adjacent positions that are always in close proximity to each other. Even in the younger, mostly vegetative state, the resolution was not high enough to make out specific compartments of the genome, even though some areas of heightened interaction frequencies can be observed. The resolution was much lower in the older sample that has progressed further in the developmental cycle. This might be an indicator of different chromatin states that could be present in cells that are only generated during sexual development. Strong horizontal and vertical lines were detectable in the deletion mutant that appeared to indicate higher interaction frequencies originating from a 600 kb are on chromosome 2 and were subsequently shown to be caused by a duplication of a region on chromosome 2.
B. Whole genome sequencing of *S. macrospora* Δasf1 confirmed the presence of a duplication in a region of around 600 kb on chromosome 2. The alignment of the reads from sequencing of the mutant genome to the wild type reference genome shows that the duplication consists of two parts, indicating either two separate duplication events or the loss of the internal area of the duplicated region. The duplication contains more than 100 genes (Supplemental Table 8).

1079 **C.** Schematics for a putative duplication on chromosome 2 of *S. macrospora* Δasf1. Whole genome
1080 sequencing proved the presence of a duplication. To test our hypothesis of a tandem duplication with
1081 an internal loss event, PCR tests with primers amplifying the genomic borders in the wild type or the
1082 newly created, duplication-specific junctions were designed. While the wild type should only yield PCR
1083 products for the external borders of the area of interest (asf1_dupl1 x asf1_dupl2, asf1_dupl3 x
1084 asf1_dupl4), strains possessing a tandem duplication should also generate products for the new
1085 junctions of the duplicated area (asf1_dupl3 x asf1_dupl2) and of the internal region lost in the
1086 duplication (asf1_dupl5 x asf1_dupl6).
1087